ABSTRACT

STIFFNESS OF VASCULAR SMOOTH MUSCLE CELLS FROM AGED PRIMATES MEASURED USING RECONSTITUTED TISSUE MODEL

by
Shilpa Nagendra

Increased stiffness of the aorta is an important detrimental change that occurs with aging. Most previous research has implicated stiffening of the extracellular collagen matrix with age. The study reported in this thesis focused instead on the potential contribution from stiffening of the vascular smooth muscle cells (VSMCs) with age.

VSMCs previously obtained from young and old monkeys (macaca fascicularis) were seeded into a collagen gel to form a reconstituted tissue. The aim of this study was to quantitatively characterize the mechanical properties of this reconstituted tissue model via uniaxially stretching each ring to defined levels of strain. The total stiffness of the reconstituted tissue was divided into the sum of two components termed "Active" and "Passive" representing the mechanical contributions of the cell and matrix respectively. The passive component was obtained from measurements following biochemical treatment that abolished cellular, actin-dependant force. The active component was obtained by subtracting the passive component from the total stiffness. This approach indicates that there was no significant difference in VSMC active stiffness between young and old female monkeys as opposed to noticeable difference in VSMC stiffness seen with aging in male monkeys [in a separate study]. This gender difference may be related to observations in the literature indicating that female mammals are relatively cardiovascularly protected by estrogen hormone.

STIFFNESS OF VASCULAR SMOOTH MUSCLE CELLS FROM AGED PRIMATES MEASURED USING RECONSTITUTED TISSUE MODEL

by
Shilpa Nagendra

A Thesis
Submitted to the Faculty of
New Jersey Institute of Technology
in Partial Fulfillment of the Requirements for the Degree of
Master of Science in Biomedical Engineering

Department of Biomedical Engineering

January 2010

APPROVAL PAGE

STIFFNESS OF VASCULAR SMOOTH MUSCLE CELLS FROM AGED PRIMATES MEASURED USING RECONSTITUTED TISSUE MODEL

Shilpa Nagendra

1/15/10

Dr. William C Hunter, Thesis Advisor — Date
Professor of Biomedical Engineering, NJIT

1/15/10

Dr. William C. VanBuskirk, Committee Member — Date
Distinguished Professor of Biomedical Engineering, NJIT

1/15/10

Dr. Cheul H. Cho, Committee Member — Date
Assistant Professor of Biomedical Engineering, NJIT

BIOGRAPHICAL SKETCH

Author: Shilpa Nagendra

Degree: Master of Science in Biomedical Engineering

Date: January 2010

Major: Biomedical Engineering

Undergraduate and Graduate Education:

- Master of Science in Biomedical Engineering,
  New Jersey Institute of Technology, Newark, NJ, 2010

- Bachelor of Engineering in Medical Electronics,
  BMS College of Engineering, Bangalore, India, 2006

For my parents, my grandmother and my loved ones

ACKNOWLEDGMENT

I would like to express my gratitude to all those who gave me the possibility to complete this thesis. I am deeply indebted to my advisor Dr. William Hunter whose help, stimulating suggestions and encouragement helped me in all the time of research for and writing of this thesis

I want to thank Dr. Stephen Vatner, for giving me permission to commence this thesis in the first instance, to do the necessary research work and to use departmental data. I would also like to express my sincere gratitude to the members of my review committee, Dr Cheul H. Cho and Dr. William C.Van Buskirk for their presence, support and diligence during this time.

I am obliged to Meredith Gansner, Lo Lai, Bei You, Misun Park and Hui Ge for their molecular biological expertise and for providing me with great laboratory knowledge. I have furthermore to thank Dr. Hongyu Qiu for her continuous support. She encouraged me to go ahead with my thesis and made my time at the University of Medicine and Dentistry of New Jersey one of the most valuable, enriching experiences of my academic career.

TABLE OF CONTENTS

TABLE OF CONTENTS
(Continued)

LIST OF TABLES

LIST OF FIGURES

LIST OF FIGURES
(Continued)

Figure **Page**

CHAPTER 1

INTRODUCTION

This thesis focuses on potential sources of the change in aortic mechanical stiffness with age. Aortic stiffness is known to increase due to changes in extracellular matrix collagen with age. This thesis specifically investigates another potential source of altered stiffness- the potential role of changes in cell stiffness with age. To study this question, the experimental work performed for this thesis uses a novel approach where vascular smooth muscle cells from old and young animals are seeded into a collagen gel to form a reconstituted tissue. The stiffness of this reconstituted tissue is then measured, and the contribution of cell stiffness to the overall tissue stiffness is then separated out.

Tissue models reconstituted from cells and extracellular matrix (ECM) components provide simplified biological systems to study cell-matrix interactions in wound healing and tissue development[1]. Measurements of tissue stiffness introduce an additional dimension, revealing mechanical functions of matrix components and cellular structural systems such as the cytoskeleton. Stiffness measurements can also probe mechanical interactions between cells and ECM, and mechanisms of tissue remodeling in development and wound healing. Moreover, characterization and control of the mechanical properties and functions of reconstituted tissue equivalents are essential tasks for practical applications of tissue engineering.

1.1 Importance of Aortic Stiffness

The term "aortic stiffness" is widely used and has been variably defined in literature[2]. Increased stiffness of the aorta, the main systemic artery of the heart, was reported to be a

predictor of cardiovascular morbidity and mortality. In general, arteries serve a dual role of conducting blood to the peripheral tissues and buffering the pressure pulsations that are an accompaniment of intermittent ventricular pumping. Loss of this function accounts to increased pulse pressure (PP), which adds load on the heart and damages the large and small vessels as well[3]. Pulse pressure may be increased because of larger forward pressure wave or an earlier or larger wave reflection. Stiffening in the aorta accounts for most of the increase in pulse pressure that is seen with aging and in hypertension. Therefore, aortic stiffness is a key variable that should to be assessed.

Aortic stiffness is associated with left ventricular hypertrophy and abnormal diastolic relaxation, which may give rise to heart failure with preserved left ventricular systolic function. Aortic stiffness is also associated with increased Coronary Artery Diseases, adding to the propensity for catastrophic cardiovascular events and poor outcomes[4].

Age, weight and gender are important and confounding determinants of aortic stiffness. Increased aortic stiffness must raise the probability of an adverse outcome[5]. To address this issue, we examined the aortic stiffness in aging monkeys, focusing on the contribution to stiffness from Vascular Smooth Muscle Cells (VSMCs). Whether enhanced aortic stiffness is a risk factor contributing to the development of cardiovascular disease or a marker which indicates the presence of cardiovascular disease is a matter of debate. A study in Chinese and Australians [6] has suggested that morphological and structural alterations of the aorta may be influenced by both environmental and genetic factors, suggesting that changes in biomechanical properties of major arteries may precede the development of clinically overt disease.

A better understanding of factors that contribute to increased aortic stiffness may provide a useful starting point for formulating strategies aimed at preventing or reducing aortic stiffening.

It will be important to determine whether reduction in stiffness with pharmacological agents can be achieved in patients, and if so whether this is proved efficacious in reducing coronary events. The cellular contribution to stiffness maybe more easily reduced by pharmacological means.

As the aorta becomes stiffer, it cannot contribute to forward flow as readily and cannot expand easily to accommodate blood being ejected by the heart. In addition, pressure waves travel faster in stiffer aortas, so pressure waves are reflected back in older adults than in younger adults and thus increases the afterload on the heart. The lack of reflections in diastole also reduces coronary artery filling.

1.2 Importance of Extracellular Matrix Stiffness

The extracellular matrix (ECM) is a dynamic structure that provides a physical framework for cells within connective tissues, imparts signals for development, tissue homeostasis and basic cell functions through its composition and ability to exert mechanical forces. The ECM is composed of 3 major classes of biomolecules:

- Structural proteins: collagen and elastin
- Specialized proteins: fibronectin, fibrillin, laminin
- Proteoglycans: these are composed of a protein core to which are attached long chains of repeating disaccharide units termed of glycosaminoglycans (GAGs) forming extremely complex high molecular weight components of the ECM.

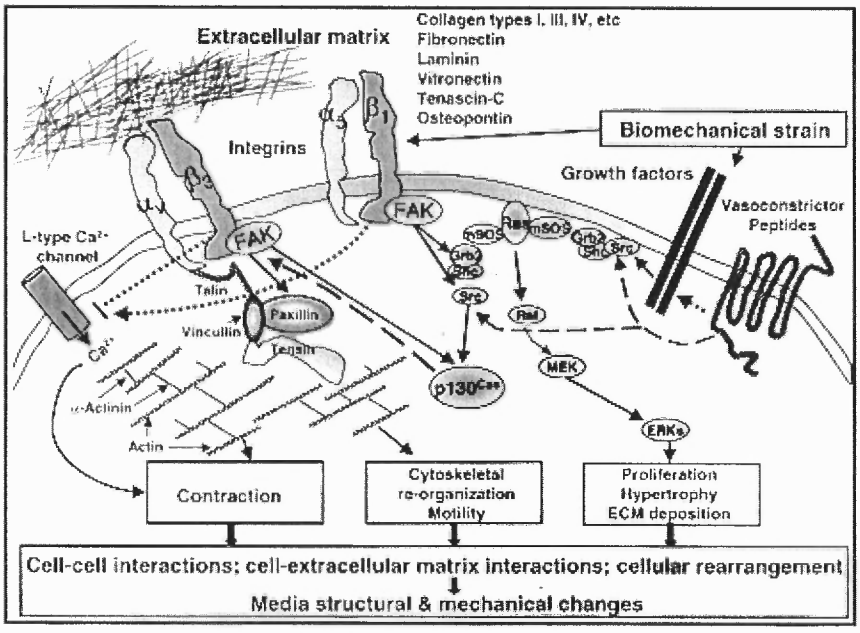

Figure 1.1 Schematic demonstration of associations between extracellular matrix (ECM) proteins and integrins on the smooth muscle cell surface[7].

Collagen is the most common protein in the human body, and is the major component of the extracellular matrix that provides the required tensile strength in tissues [2]. Therefore, it is natural that collagen is used as a scaffold for developing artificial materials in tissue engineering, particularly for blood vessel grafts where the cells are dispersed into a collagen-based cell suspension and cast into gels. Experiments found that in collagen gels populated with certain cells, contraction would occur. This contraction phenomenon exclusively occurs when collagen gel is applied as a scaffold in the above applications of tissue engineering. It is obvious that the mechanical properties of the contracted collagen gels for use as a scaffold are of significance.

This process is thought to be related to tissue remodeling and is characterized as accumulation of the collagen matrix by integrins in the vicinity of embedded cells with the resulting traction finally sustained by the cytoskeleton. Previous studies tested the

mechanical properties of rat collagen gels contracted by human fibroblasts[8]. It was found that gels contracted to about 1% of their initial volume. The stress–strain curve presented typical characteristics as found in natural connective tissues, but the mechanical strength reached only about one-tenth that of natural tissue. It was also found that the contracted gels exhibited marked stress relaxation and cyclic creep, which means that the gel samples extended a little with every reciprocating cycle. For structural tissue engineering applications such as tissue-engineered blood vessels it is very important to enhance the strength of this structure. The existing data show that different cell types contract collagen gels to different extents. Previous studies discovered that the increased passive stiffness of the heart with aging could be attributed to the changes in ECM (extra cellular matrix) and increase in stiffness of individual aged myocytes[9]. The ECM components play a critical role in arterial stiffness with aging. In this study, tissue models reconstituted from cells and extracellular matrix (ECM) simulate natural tissues. Both cytoskeletal and extracellular matrix protein govern the force exerted by a tissue and its stiffness. From previous studies, the researchers have characterized the relative contribution of the matrix to the mechanical properties of the reconstituted model tissues. The ECM dominated the passive component. However, the dynamic stiffness increased much more rapidly at high strain for passive than active component. At high strain, at which matrix dominated the mechanical properties of the Fibroblast Populated Matrix, the dynamic stiffness of the tissue formed a linear function of the force that the tissue exerted or which is exerted on the tissue.

When the fibroblast-populated matrices are treated with CD (cytochalasin D) to disrupt the cytoskeletons, the force over the entire range of strains from 0 to 20% is

reduced as seen below. CD eliminates the active contributions, the passive component remains.

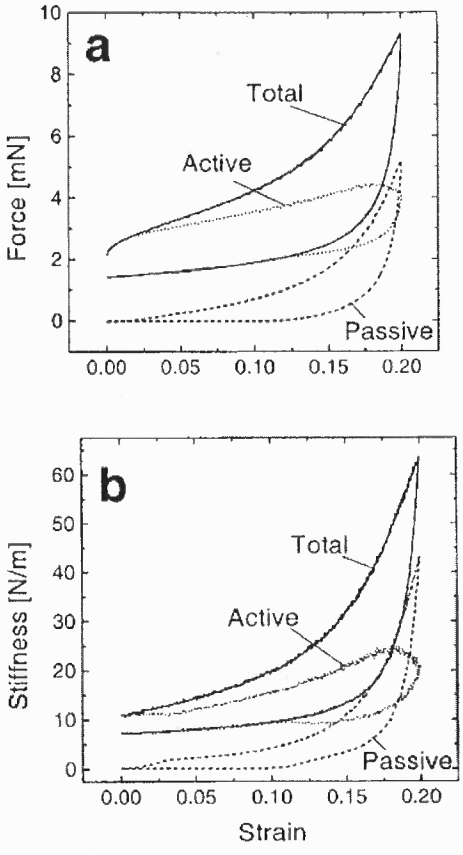

Figure 1.2 Force and stiffness versus strain for activated and Cytochalasin D-treated Fibroblast Populated Matrix (FPMs)[10].

Evidence from isolated, intact arterioles indicates that inhibition of $\alpha_5\beta_1$- and $\alpha_v\beta_3$-integrins prevents myogenic constriction in response to an acute pressure elevation. It has also been demonstrated that ligation of $\alpha_5\beta_1$-, $\alpha_v\beta_3$-, and $\alpha_4\beta_1$-integrins with ECM proteins modulates Ca^{2+} conductance through voltage-gated Ca^{2+} channels. Thus, one plausible hypothesis for the myogenic mechanism involves force transmission to sites of integrin attachment with subsequent activation of the actomyosin contractile process.

Integrins have been recognized to be important for cellular mechanotransduction. Structurally, they are a family of transmembrane proteins interposed between ECM proteins and the cytoskeleton, thus providing a mechanical connection to the extracellular environment through which mechanical forces are envisioned to be bidirectionally transmitted through focal adhesion sites.

Disruption of the actin cytoskeleton by cytochalasin D abolished the cellular force response and reduced the mechanical elasticity of the focal adhesion site in response to pulling. This is consistent with the notion that the actin cytoskeleton is the major force-bearing elastic structure in the cell. One of the most critical aspects of tissue engineering is the ability to mimic extracellular matrix scaffolds that naturally serve to organize cells and regulate their behavior[11].The ECM provides relevant micro-environmental information to the cells biochemically through soluble and insoluble mediators and biophysically through imposition of structural and mechanical constraints. To date, significant advances have been made in our understanding of how specific molecules of the ECM affect fundamental cellular responses. However, less is known regarding the mechanisms by which mechanical properties of the ECM influence cell behavior[12]. Likewise, the mechanisms by which the ECM transduces force and deformation from the macro-level tissue-organ to the micro-level cell-ECM remain to be elucidated. In this way, the physical state of the ECM, not just its molecular composition, provides the basis of cell-ECM interactions and must be considered in the design of new and improved scaffold biomaterials for tissue repair and replacement[13].

To further the understanding of ECM biomechanics and its role in cell and tissue dynamics, we have developed an experimental approach in which micro-structural and subsequent mechanical properties of a simplified model of the ECM can be controlled.

Our approach involves preparation of three-dimensional matrices from purified type I collagen. Of the many component molecules of the ECM, type I collagen is the most abundant within connective tissue structures, including tendon, ligament, dermis, and blood vessel, and is the primary determinant of tensile properties. In addition, type I collagen exhibits the ability to polymerize and form complex, 3-D supramolecular assemblies in vitro, a process known as ''self-assembly.'' Collagen fibrils formed in vitro have structural similarities to those formed in vivo and have been used extensively as a model system for understanding the collagen assembly process[13]. Collagen fibril dimensions and organization can be varied by adjusting parameters of the polymerization reaction ~i.e., collagen concentration, pH, and ionic strength[12]. Taken together, these characteristics of type I collagen make it an ideal biologically derived polymer for scaffold design. In fact, a number of biomaterials have been fashioned from type I collagen for restoration and reconstruction of specific tissues and organs. Likewise, 3-D collagen matrices have long been used as scaffolds for the culture of cells in vitro. Such in vitro systems have been shown to support a more in vivo like cellular phenotype and function and are instrumental in the study of the mechanisms involved in cell-ECM interactions [14].

Proposed relationships between collagen fibril morphology and the mechanical behavior of collagen-based tissues, scaffolds, extruded fibers, and matrices have been

documented in a variety of contexts. Parry correlated specific structural features of collagen.

1.3 Significance of Vascular Smooth Muscle Cell Stiffness

Vascular smooth muscle as the name suggests is a type of smooth muscle found in the blood vessel wall. Its primary rather fundamental mechanism is to contract and relax to changes in intralumenal pressure thereby redistributing blood to areas within the body. Arterial vessel wall is composed of three cellular layers. From the luminal side outward, the first layer is the intima in which the edothelium resides along with cells of smooth muscle cell origin called intimal Vascular Smooth Muscle Cell (VSMCs). The 2nd layer which is the medial layer is primarily comprised of the smooth muscle cells that are specialized as contractile cells to control the lumen diameter.

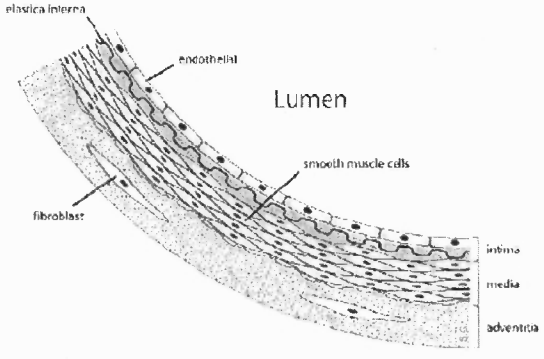

Figure 1.3 Anatomy of an artery[15]

The process of switching from the contractile/differentiated mode to a proliferating/synthetic cell type has come to be known as Phenotypic Modulation. The migration and proliferation of Vascular Smooth Muscle Cell (VSMCs) leads to the formation of atherosclerotic lesions and restenosis of arteries, one of the leading causes of

cardiovascular disorders. *Hordes Garcia et al* For example, VSMC residing in the media migrates to the intima where they proliferate, resulting in neointimal thickening.

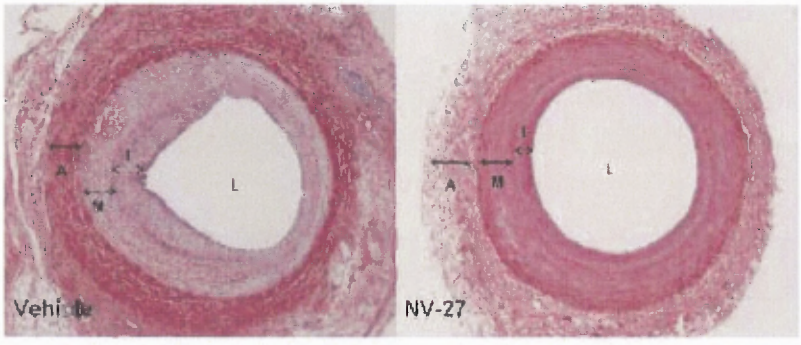

Figure 1.4 Neointimal thickening of artery[16]

Since VSMC is the major cell type found in the arterial system of animals, their study is of utmost importance in cell mechanics. Particularly in mechanotransduction, where we study the basic mechanism in which vascular smooth muscle contracts in response to increased intralumenal pressure or relaxes in response to decreased pressure. Perturbation in this intralumenal pressure triggers contraction in VSMC and this contractile force thereby exerts itself onto the ECM (extracellular matrix) it is enclosed within.

Previous studies have discovered that the increased stiffness of the vessels with aging could be attributed both to the extracellular matrix (ECM) and increase in stiffness of individual aged myocytes.

However, using primary cell cultures for study of Vascular Smooth Muscle Cell (VSMCs) proliferation rather than whole tissues has its own advantages. Basically, such cultures provide large amount of biological material for studies. Secondly, there are

replicates of a single cell type by which experimental variables are compared, in contrast to diverse cell populations in complex whole tissues. Negative aspect is that over time cultured cells are modified and lose receptors as well as cell specific markers.

An important aspect to be considered in VSMC culture is to retain as closely as possible, the morphology and function of their counterparts *in vivo*. Accordingly, one of the key aims for this thesis is to determine if the mechanical properties of VSMCs change with age such that they contribute to increased vascular stiffness with aging. Our primary focus is on the cell-matrix mechanics of reconstituted model tissue. Understanding characterization and control of mechanical properties of these reconstituted tissues from cells and extracellular matrix are essential for tissue engineering applications.

1.4 Use of Reconstituted Tissues

Reconstituted tissue models are useful and powerful systems for studying extra-cellular matrix and cell mechanics. The production of tissue constructs from reconstituted tissue models is important in supplying equivalents that can be used to replace diseased/damaged tissues. In particular, fibroblasts that contribute to wound healing and development of tissue naturally remodel the extracellular matrices in which they are embedded. Therefore these remodeling parameters could be used to produce tissue constructs with desired properties.

Quantitative measurements of force by these models provide a powerful approach in studying the mechanisms of force regulation in non muscle cells[10]. Measuring tissue stiffness reveals an additional dimension of mechanical functions of matrix and cytoskeleton components respectively. Stiffness probes mechanical interactions between

the cells and extra-cellular matrix. Characterization and control of mechanical functions of reconstituted tissue are essential for practical applications of tissue engineering.

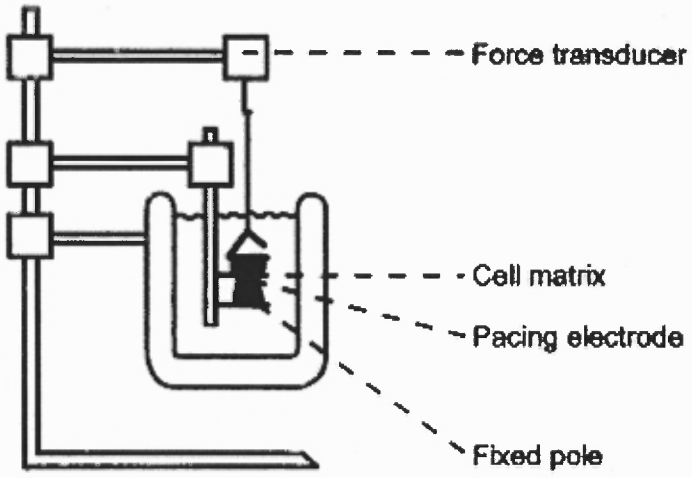

Figure 1.5 Photograph of Fibroblast Populated Matrix (FPMs) ring connected to force transducer[17, 18]

Cells remodel extracellular matrix during tissue development and wound healing. Similar processes seem to occur when cells stiffen and compress collagen made gels[19]. An important task for cell biologists, biophysicists, and tissue engineers is to have an understanding in these remodeling processes to produce tissue constructs that mimic the structure and mechanical properties of natural tissues *in vivo*. This requires an understanding of the mechanisms by which this remodeling occurs. Quantitative measurements of the contractile force developed by cells and the extent of compression and stiffening of the matrix describe the results of the remodeling processes. Not only do forces exerted by cells influence the structure of the matrix but also external forces exerted on the matrix can modulate the structure and orientation of the cells. The mechanisms of these processes remain largely unknown, but recent studies provide clues about the regulation of cellular functions during remodeling.

In Fibroblast Populated Matrix (FPMs) studied in previous works the cells have compressed the matrix to an extent thereby stiffening the tissue and establishing a basal contractile force[17]. However, this process is similar to the natural processes that occur during tissue development and wound healing. Long term goal of reconstituted tissue models is to study the mechanical functions of cytoskeletal proteins.

1.5 Specific Aims of this Thesis

An increase in vascular stiffness is a fundamental component of aging with broad significance for health care. The effects of aging on arterial stiffness are relatively protected in older women. However, very little is known about mechanics, which rely on rodent models. Relatively novel approach of this study is to utilize a primate model of aging, which is closer to clinical situation. And this is of particular importance as the extent to which these data can be extrapolated to humans is limited both by species differences, but also by the marked differences in lifespan over which changes in vascular stiffness develop, i.e., 2-3 years in rodents vs. 60-80 years in humans. Studies of gender differences with aging are even more difficult in rodents as they do not go through menopause and that the estrogen levels never decline in very old rodents. It is considered that the non-human primate is the best model to study gender differences in aging, since changes in menstruation and hormonal changes parallel those in older human females.

Therefore, the specific aim of this thesis is to investigate the potential difference in Vascular Smooth Muscle Cells (VSMCs) contribution to increasing vascular stiffness within the female population of the Macaca Fascicularis with age. This is done using a reconstituted tissue model whereby the mechanical contributions of the cell- matrix

interaction can be studied. This study primarily focuses on how the VSMCs mechanical contribution influences the whole dynamics of the tissue model. We will quantitatively characterize mechanical properties of tissue constructs via uniaxial stretch measurements.

CHAPTER 2

MATERIALS AND METHODS

2.1 Animal Model

The experimental work conducted for this thesis used isolated Vascular Smooth Muscle Cells (VSMCs) cryopreserved after isolation from experimental animals. These cells were obtained from the following age-varied sets of animals. Young female (age, 4-8 years), old female (age, >18 years) monkeys (Macaca Fascicularis) were studied. The old females were either premenopausal (still cycling) or perimenopausal (irregular cycles), which is consistent with prior reports in this species[20]. Young monkeys were second generation in captivity, and old monkeys were feral animals captured at the age of 5 to 7 years old and kept in captivity for 12 to 15 years. All the animals come from the same species of Philippine monkey and were bred in captivity at the Simian Conservation Breeding and Research Center, Inc (Manilla, Philippines)[21]. The monkeys were fed a primate diet containing 5% to 6% fat, 18% to 25% protein, and 0.2% to 0.3% sodium chloride. The animals used in the present study were maintained in accordance with the Guide for the Care and Use of Laboratory Animals (National Institutes of Health 83–23, revised 1996).

2.2 Isolation of the Cells

The animals were anesthetized and sacrificed according to protocols approved by the UMDNJ comparative medicine committee. Vascular Smooth Muscle Cells were extracted from the medial layer of the aorta through natural migration to a cell culture

plate[22]. About 2 cm of thoracic and abdominal aorta were isolated and placed in a petri dish with 10-15 ml of PBS (phosphate buffered saline). The outer layer (adventitia) and inner layer (intima) were removed using forceps and the remaining (medial layer) was placed in a 100 mm cell culture dish and cut into small pieces of about 1 mm in size. The pieces were further spaced about 5mm apart and then covered with 3 to 4 ml of adhesion medium [(Dulbecco's Modified Eagle Medium, DMEM, 20% Fetal Bovine Solution(FBS) + 1%Penicillin Streptomycin (PS)]. The dish was then placed in a 5% CO^2 incubator (37° C) and the culture medium was changed every day. Once the Vascular Smooth Muscle Cell (VSMCs) were visible (7-10 days), the pieces of aortic medial tissue were removed and the culture medium was replaced with a slightly different culture solution (DMEM, 10%FBS + 1% PS).

2.2.1 Cryopreservation of original animal cells

The medium was aspirated and culture plates were rinsed once with Phosphate Buffered Saline solution. To detach cells from the plate, 3ml of trypsin was added, followed by incubation at 5% CO_2 and 37° C for 10 minutes. Then 4 ml of culture solution was added and the resulting cell suspension was transferred to a 15ml tube and centrifuged at 1000rpm for four minutes. Afterwards the supernatant was discarded and 1ml of freezing medium (DMEM, 30% FBS, 10% DMSO) was added. The pellet was re-suspended and transferred to a 1.5ml freezing tube. The tubes were placed on ice for 20 minutes and then overnight at -80° C. After this preparation these cells were ready for shipping from Manilla to Newark, NJ and for long term storage (~ 1 year) at -80° C at the University of Medicine and Dentistry in Newark, NJ.

2.3 Culture to Expand Cell Numbers

The cryo-preserved cells from the young and old female primates were a valuable resource. In order to make tissue constructs from these cells, the numbers of each type of cell had to be amplified from smaller original samples of each type. This involved culturing of the VSMCs through several passages to enable them to proliferate up to 90% confluence at each stage. The following steps involved in culturing the VSMCs:

2.3.1 Thawing

To conduct further cell culturing, the cells were taken out from the freezer set at -80^{0}C and thawed. The freezing vials were taken out from the freezer and put into the incubator for 4 minutes. The cell suspension was aspirated and placed into a tube with 5ml of Vascular Smooth Muscle Cell medium. The pellet cells were then centrifuged. After centrifugation, the supernatant was aspirated, 5ml of Vascular Smooth Muscle Cell (VSMCs) medium was added and the cells were re-suspended. The suspension was taken into a 100 ml petri dish and 5 ml VSMC medium was added. The dish was placed into a 37°C, 5% CO_2 incubator until the cells proliferated to 90% confluence.

2.3.2 Passaging of cells/ Subculturing

Passaging of cells is basically subculturing of cells. When the cells had reached more than 90% confluence in their petri dish, they were passaged so as to split their numbers into two new groups. Each of these could now grow towards 90% confluence on their own. When the cells have reached a suitable confluency, they are split into two daughter groups. Basically the cells are subcultured into the next generation. The following were the steps involved in splitting the cells. The medium was aspirated and 1 ml of trypsin

was added. After a minute the contents were pipetted out and again 2 ml of trypsin was added and allowed to cover all the cells evenly.

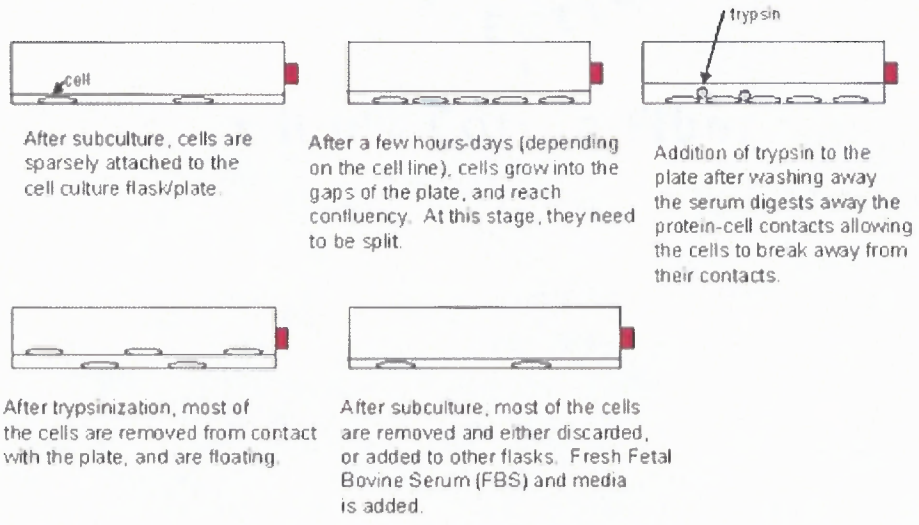

Figure 2.1 Steps involved in splitting of cells[23].

trypsin was added and allowed to cover all the cells evenly. After which the dish was put back into the 37°C 5% CO_2 incubator for 5-10 minutes (checking the cell every 2 minutes to make sure all cells are detached).Then 4 ml of growth medium was added into the trypsinized dish and the cells were re-suspended into equal amounts of 3 ml and placed into two petri dishes with added 5ml of growth medium in each. Each dish was then placed into the 37°C 5% CO^2 incubator, thereby passaging the cells.

2.4 Construction of Cellularized Tissue Rings

As explained earlier in this chapter, Vascular Smooth Muscle Cells (VSMCs) were isolated from young and old female monkey aortas. Cells were maintained in Dulbecco's modified Eagle's medium (DMEM) supplemented with 10% fetal bovine serum (FBS), 50 units/ml penicillin and 50 mg/ml streptomycin (P/S). Reconstituted tissues were

fabricated as described next using a method first described in [8, 9]. Briefly, VSMCs from passages 2–8 were added to a collagen solution containing monomeric rat tail tendon collagen (Upstate Biotechnology Inc., Lake Placid, NY) neutralized with 0.1N sodium hydroxide (NaOH) and mixed with 2× concentrated DMEM. The final solution contained 0.6 mg/ml collagen and 7.5 million cells/ml. Either 250 µl or 500 µl of this cells + collagen solution was poured into cylindrical molds (inner diameter = 7 mm) containing an inner mandrel (diameter=4.5 mm). The molds were made from Teflon and are shown in figure below.

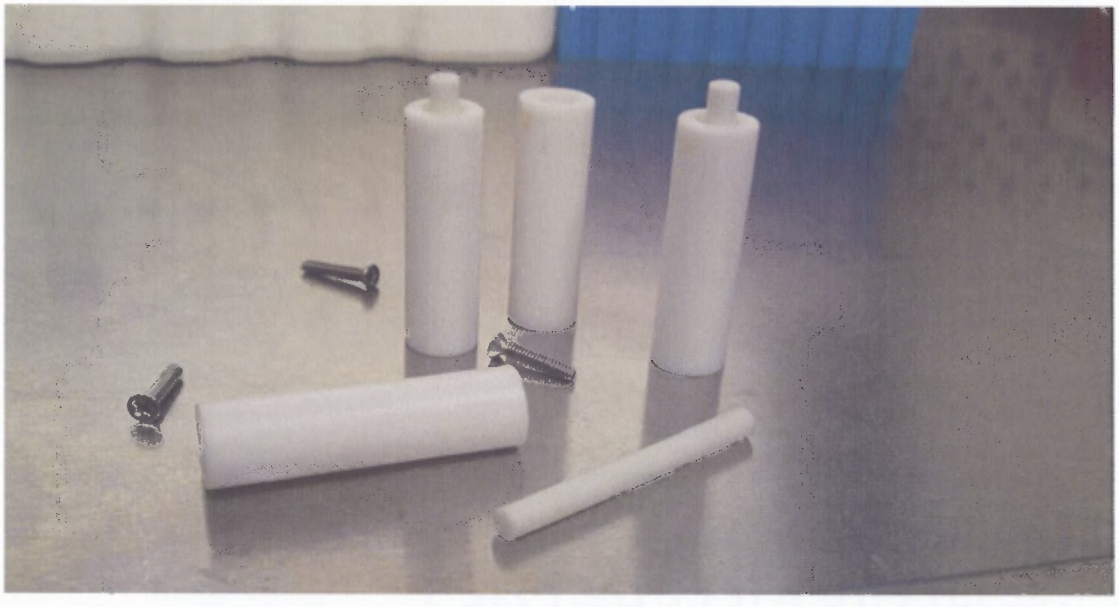

Figure 2.2 Ring Molds – cylinder + inner mandrel

After one hour of incubation at 37° C and 5% CO_2, the solution gelled and the molds were then filled with incubation medium containing DMEM supplemented with 10% FBS and P/S. The Vascular Smooth Muscle Cells (VSMCs) were captured within the hydrated collagen gel. The collagen gel formed a ring between the inner wall of the cylindrical well and the central mandrel. During subsequent culture over two days, the

cells compressed this ring, reducing its volume many fold. The ring could then be removed from the mandrel and mounted on the measuring instrument as described below.

The figure on the next page summarizes the steps used to produce rings of reconstituted tissue containing VSMCs in a collagen gel. This figure describes the process for reconstituting tissues containing fibroblasts instead of VSMCs, but the same process was used for VSMCs. In detail (refer to panels shown in the figure):The VSMCs and monomeric collagen (*a*) are mixed in DMEM at pH 7 (*b*). This solution is poured into casting wells containing a central mandrel (*c*) and polymerized at 37°C (*d*). The wells are incubated (*d*) for few days, during which the cells compress and remodel the collagen matrix. After the incubation the mandrel is removed from the well (*e*) and the reconstituted tissue-ring is removed gently from the mandrel (*f*). The tissue-ring is then connected to the force-measuring apparatus (an isometric force transducer) and a micrometer (not shown) that controls the tissue strain (*g*). In our study, the micrometer was adjusted manually instead of using a computer-controlled stepper motor.

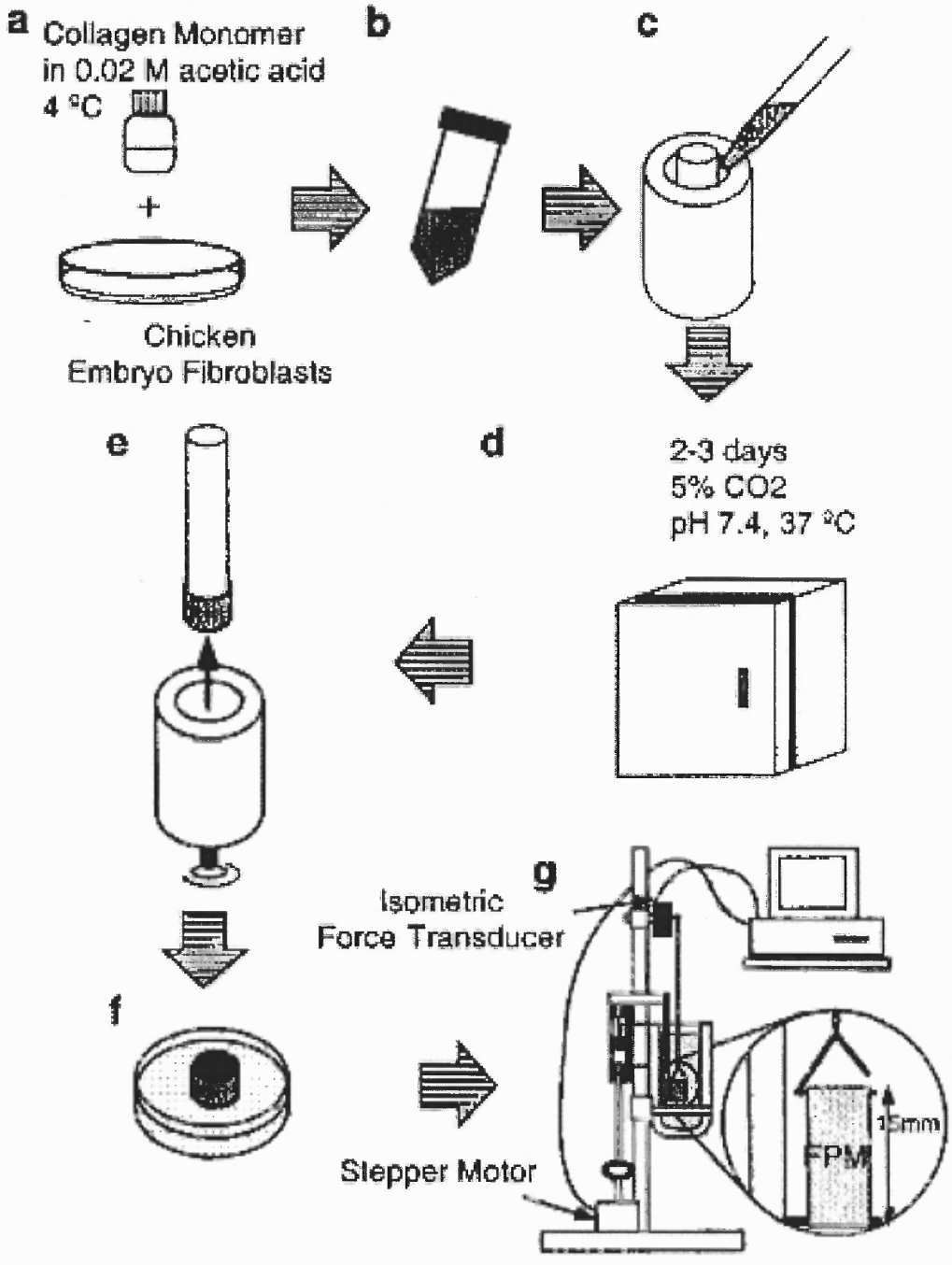

Figure 2.3 Schematic of methods to prepare and measure fibroblast populated matrices (FPMs). [6] Similar techniques were used to reconstruct tissue rings using VSMCs. In our study.

2.5 Apparatus for Mechanical Testing and Measurement

After 2 days of incubation the mandrel was removed from the well. The width of the tissue ring as it extended along the mandrel was measured using a linear scale calibrated in millimeters. Next the ring was removed from the mandrel [8] using a gentle jet of culture medium. It was then looped over a triangular hook connected to an isometric force transducer (model 52-9545, Harvard Apparatus, South Natick, MA) by a chain. The ring was also looped over a horizontal bar connected to a sliding element that was later used to stretch the tissue ring. The figure below shows a similar setup from a collaborating laboratory as reported in the literature [[24]]. In our setup, however, the micrometer drive was altered manually – as described in the next paragraph – and there was no stepper motor.

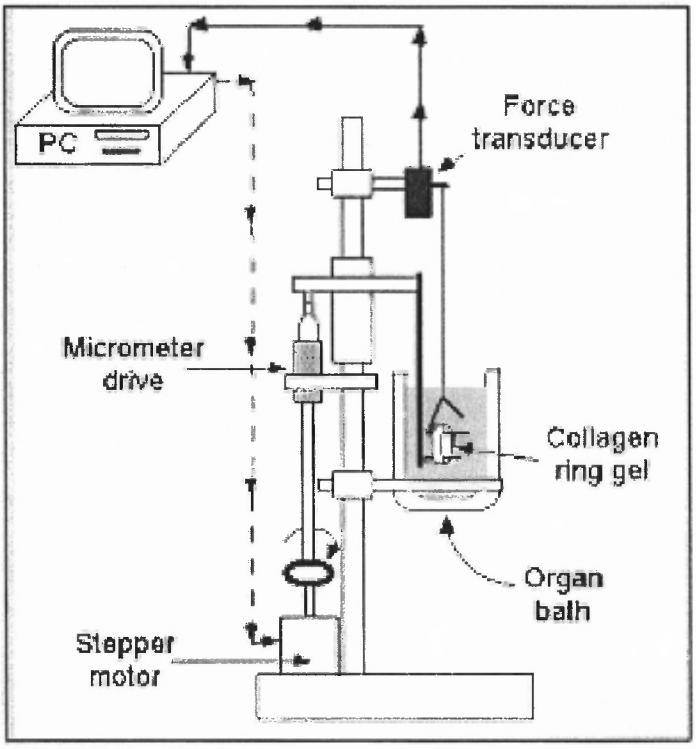

Figure 2.4 Details of loading arrangement for one ring-shaped gel specimen[17].

Stretch of the ring was produced by downward displacement of the lower bar around which the tissue ring circled (see figure). Sudden steps of a predetermined amount of strain were produced by the combination of an electromagnetic hold/release system and the micrometer, which controlled a mechanical stop. When the electro- magnetic system was on, it held a steel plate fixed; the lower bar was fixed to this plate, so that ring length also remained constant while the electromagnet was on. With the magnet on, the micrometer was adjusted so that a mechanical stop was lowered 0.5 mm. Then, when the electromagnet was suddenly switched off, the plate holding the lower bar fell 0.5 mm to the mechanical stop, and the ring was thus suddenly stretched by 0.5 mm.

After mounting the ring, the mechanical system was initially adjusted so that the distance between the two bars was 3.5 mm. This was considered the "unloaded" lengths of the ring (Lo) to which all displacements were referred to calculate tissue strain. Note that at L_o the ring was considerably shorter than its equivalent "length" while it was incubating on the mandrel. Since the mandrel diameter was 4.5 mm, its circumference was 14.1 mm, which would correspond to a ring spanning a separation between the bars of 7 mm. However, recall that the ring compressed itself against the mandrel; hence, its unloaded length was considerably shorter than its length when it was around the mandrel. For consistency, the initial ("unloaded") L_o of the tissue ring was thus chosen to be half its length when around the mandrel.

The electromagnet and micrometer system was adjusted to produce 3 successive steps of 0.5 mm each. Each step thus corresponded to a strain of 14% (0.5mm / 3.5mm). The strains applied were thus steps from 0 to 14%, from 14% to 28%, and from 28% to 42%. Only force data from the last strain step was used for mechanical analysis. The

preceding two steps were considered to provide a sort of mechanical "preconditioning" to the tissue ring.

The tissue ring was submerged in 50 ml Hepes-buffered DMEM (pH 7.4) in a thermo-regulated organ bath (Harvard Apparatus, South Natick, MA) maintained at 37°C. The figure below shows 4 of these tissue baths, each with its own electromagnetic mechanical stretching system and force transducer.

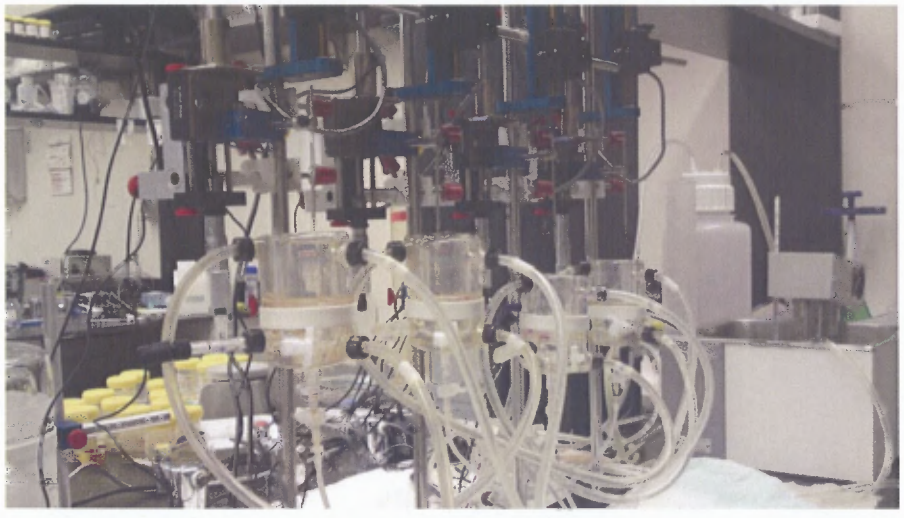

Figure 2.5 Arrangement for simultaneous mechanical testing of four ring specimens.

2.5.1 Calibration of Force

The force was calibrated according to set protocols of the software data acquisition system (NOTOCORD Systems SAS, France). Accordingly, the maximum output of 5000 millivolts was set to correspond to a mass of 5 grams hanging from the isometric force transducer. Hence, 1 gram produced 1 Volt, otherwise put forth as 1 g/V. While 'grams-force" still remains popular as a unit used in the physiological literature, we preferred to use a true SI force unit (Newtons) in our analysis. Since the force (ie, weight) exerted by a hanging 1gram mass would be 0.0098 N = 9.8 mN, we used the

calibration that 1 Volt = 9.8 mN (ie, 9.8 mN/V). When the cross-sectional dimensions of the ring were also included, we computed stresses in Pascals. Note that 1 mN/mm^2 is equivalent to 1000 Pascals.

Note that the amplifier for the force transducer had a switch on the front panel that toggled between "5g" and "0.5g". This switch set the gain of the force transducer system. At the "0.5g" setting, a small force – corresponding to the weight of a mass of only 0.5g – would produce the full scale voltage output of 5000 mV. So the gain of the amplifier would be 10 times higher at that setting. Throughout the experiments re-ported in this thesis, the switch on the force amplifier was consistently set at "5 g".

2.5.2 Zeroing of Length Measurement and Setting Initial State of Tissue Ring

The micrometer was adjusted to its "zero" position when the top of the upper (triangular) bar lined up with the bottom of the lower (stretching) bar. After moving the bars somewhat farther apart, the tissue construct was looped over the two bars. The bars were then set at a distance of 3.5 mm (relative to their "zero" position, as described above), and the tissue construct was allowed to equilibrate briefly at this length. This was considered its initial state, to which all other mechanical measurements were referred.

2.5.3 Determination of Cross-Sectional Area of Ring in Initial State

The stress we calculated was always nominal (engineering) stress. That is, the cross-sectional area used for stress calculations was the area when the ring was in its initial state. We did ***not*** calculate what is called true or Cauchy stress, which would have

required recalculating the cross-sectional area for each degree of stretch. Most stresses reported in the physiological literature use nominal (engineering) stress.

The cross-sectional area in the initial state was based on the volume of tissue in the ring. We assumed that the volume of tissue did not change from when the ring was slid off of the mandrel to when it was mounted in the mechanical apparatus with its initial length = 3.5 mm. Therefore,

$$\text{Width}_O \times \text{Thickness}_O \times \text{Length}_O = \text{Width}_M \times \text{Thickness}_M \times \text{Length}_M$$

The subscript "**O**" refers to the initial state mounted in the mechanical apparatus. The subscript "**M**" refers to the ring when it was on the mandrel.

The product ($\text{Width}_O \times \text{Thickness}_O$) gives the cross sectional area of one arm of the loop. Since both arms of the tissue loop support the force measured by the transducer, the area supporting that force (A_O) in the initial state is twice the area of each arm:

$$A_O = 2\ (\text{Width}_O \times \text{Thickness}_O)$$

A_O is the cross sectional area we will use to normalize force and to calculate stress.

Other than Width_M, which varied with each ring, all other factors determining A_O are known or assumed to be known. Length_O = 7 mm, since the total length of the ring is twice the distance between the bars in the initial state. Length_M is the circumference of the mandrel, which we will round off here to 14 mm. Thickness_M was assumed to be 0.25 mm. Solving for A_O yields

$$A_O = \text{Width}_M \times 1\ \text{mm}$$

2.6 Experimental Procedure

When the tissue ring was slack in the mechanical apparatus, the force transducer registered a small positive or negative value. Since this value was small (approx < 10% of maximum force), no attempt was made to precisely offset and zero out this force.

Three consecutive stretches were applied to the tissue ring by imposing sudden strains of 14% at each step. The force response to each step followed a stress-relaxation response, typical of a viscoelastic tissue. We waited for 120 s following each step before recording the force value at the end of that 2 min period of stress relaxation. The elastic stiffness of the tissue was estimated from the ***change in stress*** that occurred during the last of the three stretches prorated by the ***change in strain*** during that last stretch, which was always 14%, as noted above.

To determine the cellular contribution to the measured stress and stiffness, we used cytochalasin-D (CD) to disrupt the actin cytoskeleton of the Vascular Smooth Muscle Cell (VSMCs). This eliminated completely the force generated by cells and left only the force borne by the extracellular matrix (ECM). Thus, the difference between the force generated by the intact construct and the force by the ECM alone (following CD treatment) was assumed to be the force generated by the cells.

After the 3 consecutive stretches to the intact tissue ring, cytochalasin-D (2μM) was added, which lowered the tension developed. The ring was then returned to its length just prior to the final stretch, and after 120 s, the force at this baseline (for CD treatment) was observed. Then, the last 14% sudden stretch was reimposed, and after 120 s for stress relaxation, the final force was recorded.

2.7 Statistical Data Analysis

Mean values were reported plus or minus the standard error of the mean. The statistical significance of differences in quantitative measurements was determined using Student's t-test. A *P* value less than 0.05 was considered significant.

CHAPTER 3

RESULTS

3.1 Seeding of Cells into Tissue Molds

The density of cells produced by the culturing process that expanded cell numbers differed significantly between cells from young females (YF) versus old females (OF). Essentially, cells from young females had greater proliferative power, so that their density at the end of the initial cell culture process was more than double the density of cells from old females. Cell density was determined by manually counting cell samples on a hemocytometer. The table and figure below present the average cell densities observed for cells from old (OF) and young (YF) female primates.

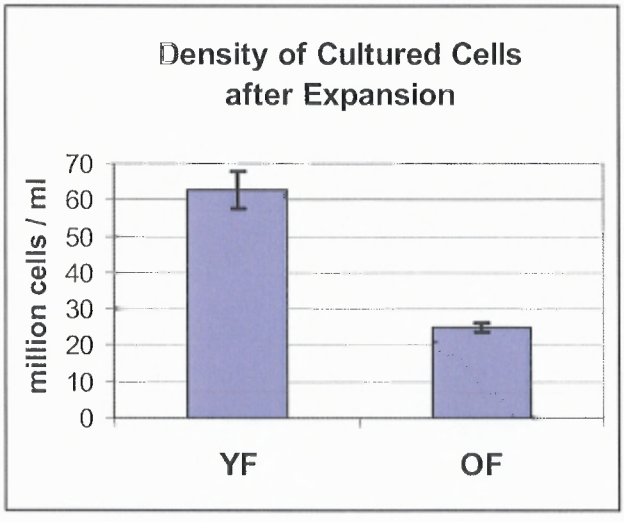

Figure 3.1 Cell Density Comparison

Table 3.1 Results of Student's t-test for Cell Density between OF and YF

		Cell Density Comparison			
	mean	sqrt n	SE	P value	Significance (P<0.05)
OF	25	3.46	1.3		
				0.0001	Significant Difference
YF	63	2.83	5. 2		

When the cells were seeded into tissue molds, this inherent difference in the density of cells achieved during the culturing process was taken into account. To achieve a less biased comparison between reconstructed tissues, the density of cells seeded into each construct was maintained constant at 7.5 million cells / ml. This implied that the volume of cell solution added to the tissue mold varied for each cell sample in accordance with the cell density measured for that sample. Table 3.2 summarizes the volumes of cell solution used for each experimental cell sample. Since the cell densities were much smaller for the OF cells, a smaller tissue construct was formed. Only a total of 250 μl of the reconstituting solution was placed into the molds for OF, while 500 μl of solution was used for YF. (Table 3.2 also shows tissue widths, to be discussed later.)

Table 3.2 Cell Volume & Density Used in Tissue Molds, and Subsequent Tissue Width

Experiment Sample	Young/ Old	Tissue Width (mm)	Cell Volume (μL)	Cell Density (million cells / ml)
1	YF	6	54	69
2	YF	6	44	85
3	YF	9	63	60
4	YF	9	49	77
5	YF	10	63	60
6	YF	12	59	64
7	YF	15	89	42
8	YF	15	84	45
1	OF	2	97	19
2	OF	3	59	32
3	OF	4	59	32
4	OF	4	92	20
5	OF	4.5	92	20
6	OF	5.3	75	25
7	OF	6.6	75	25
8	OF	7	82	23
9	OF	7.6	59	32
10	OF	8	82	23
11	OF	8	82	23
12	OF	9	75	25

3.2 Compression and Elongation of Reconstituted Tissue During Remodeling

During the two days of incubation following the initial formation of the reconstituted tissue, the contraction of the vascular smooth muscle cells around the mandrel substantially compressed the volume of the tissue gel against the mandrel. Simultaneously, the ring of tissue also extended itself up the mandrel, so that the width of the reconstituted ring enlarged. The geometry of the reconstituted tissue that develops during incubation is described in Figure 3.2 below. Initially, as the tissue gelled within the first hour after the tissue solution was placed into the mold, the thickness of the ring equaled that set by the mold, 1.25 mm. Over the next two days, contraction of the VSMCs then drove excess fluid out of the tissue, and the thickness of the tissue ring decreased substantially. Unfortunately, the lab had no means to measure the final thickness, so it was assumed that the final thickness of all rings equaled 0.25 mm. This is the average of the range 0.2 – 0.3 mm reported in the literature for similar experiments in another lab [ref]. Compaction of the tissue against the mandrel expanded the final width of the tissue ring to the values reported in Table 3.2 on the preceding page.

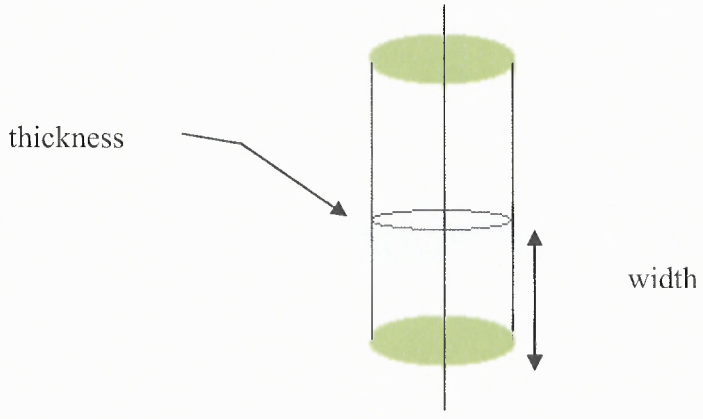

Figure 3.2 Compaction of Tissue Ring Against and Along the Mandrel

3.2.1 Test of Assumed Equal Final Thickness Using the Compaction Ratio

The thickness of the tissue ring is an important parameter that will impact subsequent calculations of tissue stress and stiffness during mechanical testing. To evaluate whether the assumption of equal thickness for all samples was reasonable, we used this assumption to estimate the compaction ratio for each tissue sample. We defined the compaction ratio as the ratio of the volume of tissue gel when first placed in the mold divided by the final volume of the tissue just before being slid off the mandrel. Final tissue volume was estimated by the product of (mandrel circumference) x (measured width of tissue ring) x (assumed thickness). The initial tissue volume was either 250 μl (for OF) or 500 μl (for YF). The results shown in Tables 3.3 and 3.4 below indicate that 1) there was no bias in the compaction ration between tissues reconstituted from old versus young cells, and 2) the average value of the compaction ratio was consistent with reports in the literature that tissue volumes typically contracted at least ~10 fold. These results allowed us to accept the estimate of tissue thickness that we had proposed.

Table 3.3 Compaction Ratios for Tissue Rings with Cells from Young and Old Females

	CompactionRatio		CompactionRatio
Young	23.58	Old	35.37
Females	23.58	Females	23.58
	15.72		17.68
	15.72		17.68
	14.15		15.72
	11.79		13.35
	9.43		10.72
	9.43		10.11
			9.31
Average	15.42		8.84
			8.84
			7.86
		Average	14.92

Table 3.4 Results of Student's t-test of Compaction Ratios

		Compaction Ratio Mean			
OF	**sqrt n**	**SE**		**Pvalue**	Significance (P<0.05)
	3.46	2.32			
				0.87	No Significant Difference
YF	2.83	1.98			

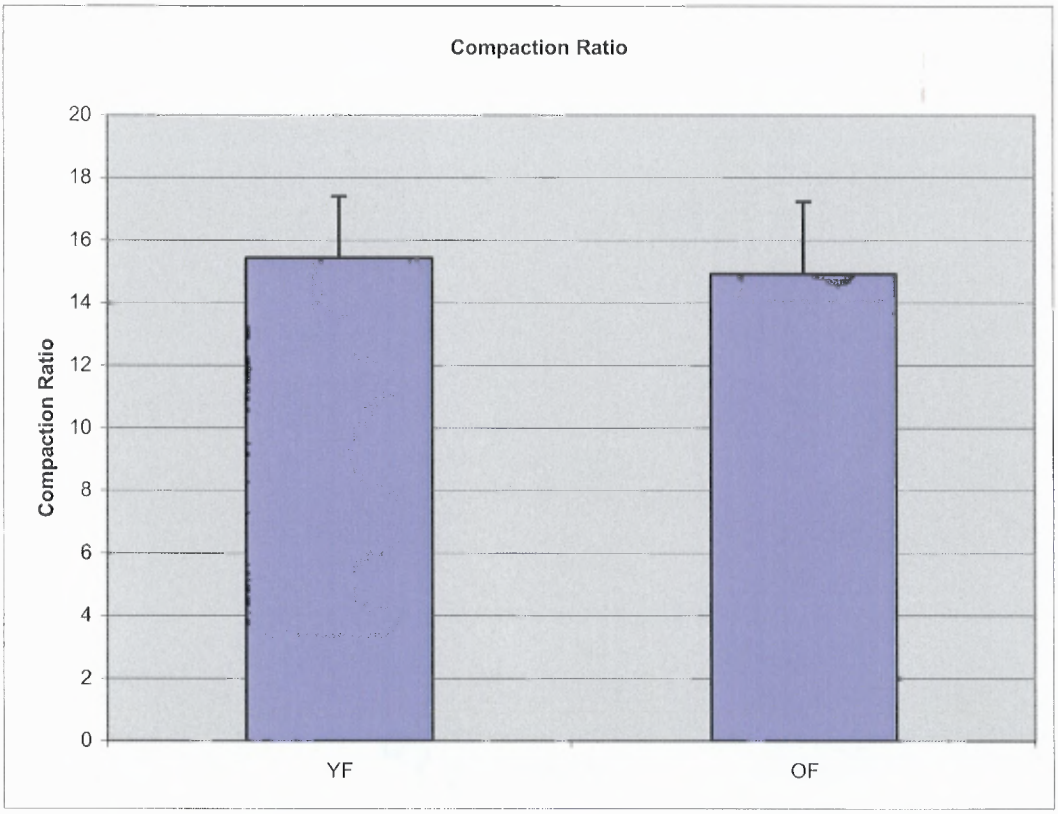

Figure 3.3 Comparison of Compaction Ratio between young and old females.

3.2.2 Contribution of Width to Tissue Stiffness

Tissue ring width is another important parameter that needs to be examined during the course of the experiments. There was quite a variation in width among the tissue constructs within either set formed from young or old cells. Nevertheless, tissue rings in the final, incubated construct were almost always wider than in the initially seeded state. (Only 1 exception in 20 experiments.) Keeping in mind the 500 μL and 250 μL volumes used to constitute the initial constructs for young versus old females, respectively, it is natural that the width of the tissue construct would be consistently greater for constructs formed from YF cells. The width in turn impacts the overall stiffness and distribution of stress in the tissue construct.

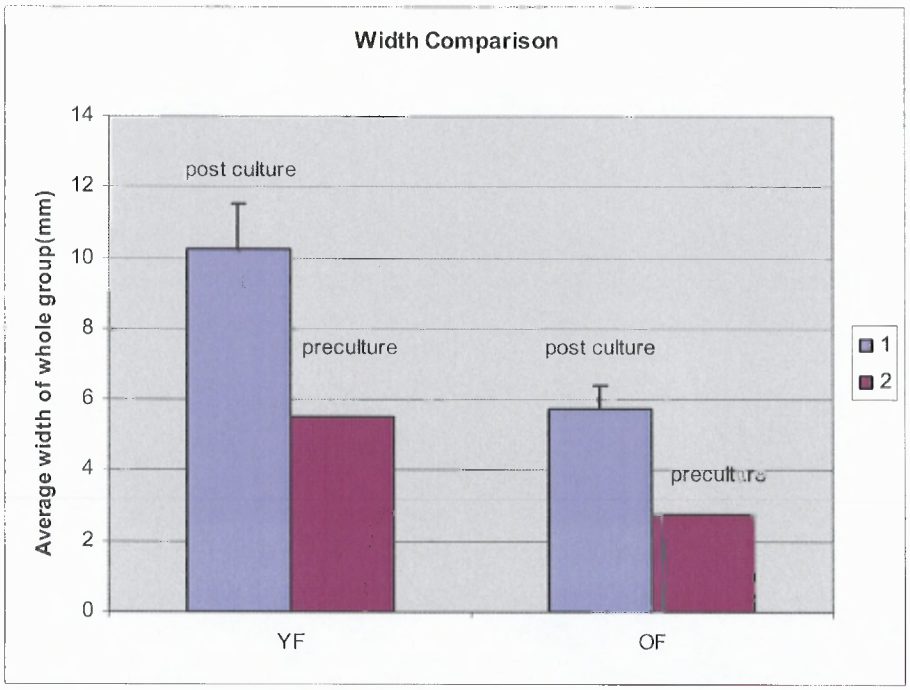

Figure 3.4 Width comparison in post and pre culture of Young Females and Old Females.

The width comparison of post and pre culture between young and old was performed and there was a considerable difference between the two as shown in Table 3.5.

Table 3.5 Width Comparison post and pre culture

	YF	OF	SE	P value
Post Culture	10.25	5.75	1.25	0.008
Pre Culture	5.53	2.76	0.65	

Table 3.6 Width of the preculture tissue

	Volume input(μL)	Annulus Area(mmsq)	Width preculture
	i μL = 1 cu.mm		
YF	500	90.3	5.54
OF	250	90.3	2.77

The width in the preculture was measured by the volume input (YF =500μL & OF=250 μL) divided by annulus area in the ring mold. The annulus area of the ring mold was the same measuring 90.3mm^2 for both YF and OF. Therefore the width pre culture was calculated as 5.54 mm and 2.77 mm for YF and OF respectively. The width for the post culture YF and OF was measured directly using a linear scale of measurement when the ring was on the mandrel. The mean width came to be 10.25 and 5.75 for YF and OF respectively. The width seemingly doubled post culture showing that 1) the cells were under tension and elongated along the mandrel and only grew is length.2) since the YF showed high values of width throws light on the high proliferating power of YF as compared to OFs. The following two tables 3.4 and 3.5 show the difference in the range of thickness between old and young female monkeys.

Table 3.7 Width of Final Constructs from Cells of Young Female Monkeys

TissVol Post	Diam	Thick(mm)	**Width(mm)**
21.21	4.5	0.25	6
21.21	4.5	0.25	6
31.81	4.5	0.25	9
31.81	4.5	0.25	9
35.34	4.5	0.25	10
42.41	4.5	0.25	12
53.01	4.5	0.25	15
53.01	4.5	0.25	15

From the tables, the higher increase in width in the YF than OF could also be attributed to the fact that the higher volume of solution added to YF for making tissue , however had enough proliferative power that they climbed up the mandrel to greater heights compared to the OF. The OFs from previous literature were known to undergo senescence , therby decreased in cell number and contributed to very little width increase as compared to YF.

Also the values tabulated from the cell density shows increase in YF density as compared to OF only reinforcing the above mentioned statement of increased width in YFs.

Table 3.8 Width of Final Constructs from Cells of Old Female Monkeys

Tissue Volume Post	Diameter(mm)	Thick(mm)	**Width(mm)**
7.07	4.50	0.25	2.00
10.60	4.50	0.25	3.00
14.14	4.50	0.25	4.00
14.14	4.50	0.25	4.00
15.90	4.50	0.25	4.50
18.73	4.50	0.25	5.30
23.33	4.50	0.25	6.60
24.74	4.50	0.25	7.00
26.86	4.50	0.25	7.60
28.27	4.50	0.25	8.00
28.27	4.50	0.25	8.00
31.81	4.50	0.25	9.00

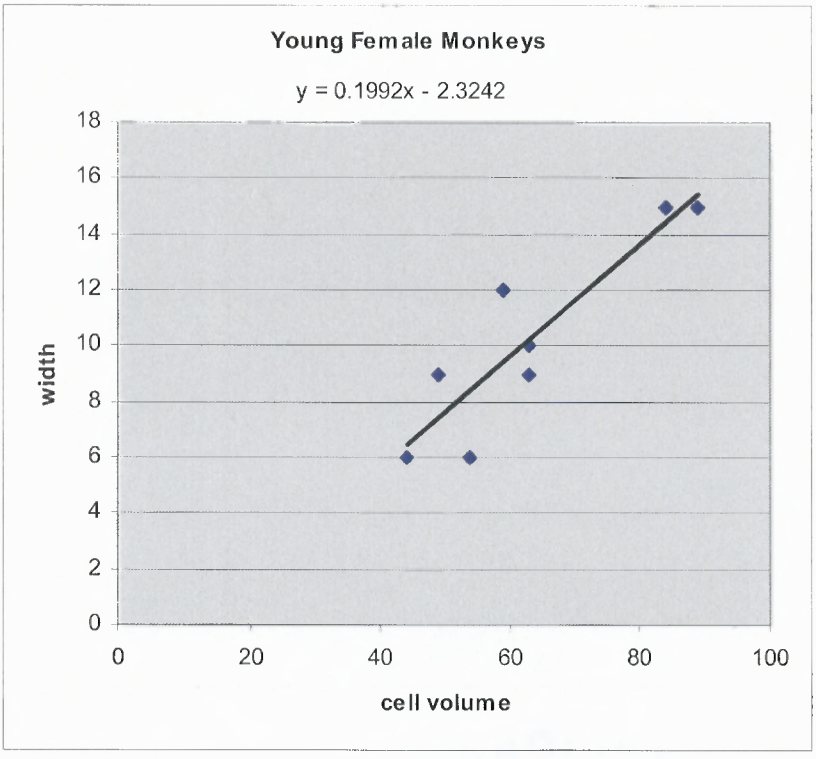

Figure 3.5 Width as a function of cell volume

For constructs formed from young cells, the graph shows a positive correlation of width with increasing volume of cell solution used to form the construct (which correlated with low cell density in the cell solution – see above). The cell volume being the control parameter is plotted on the x axis and the width variable on the y axis. However, there was no meaningful correlation between width and volume for old-cell constructs.

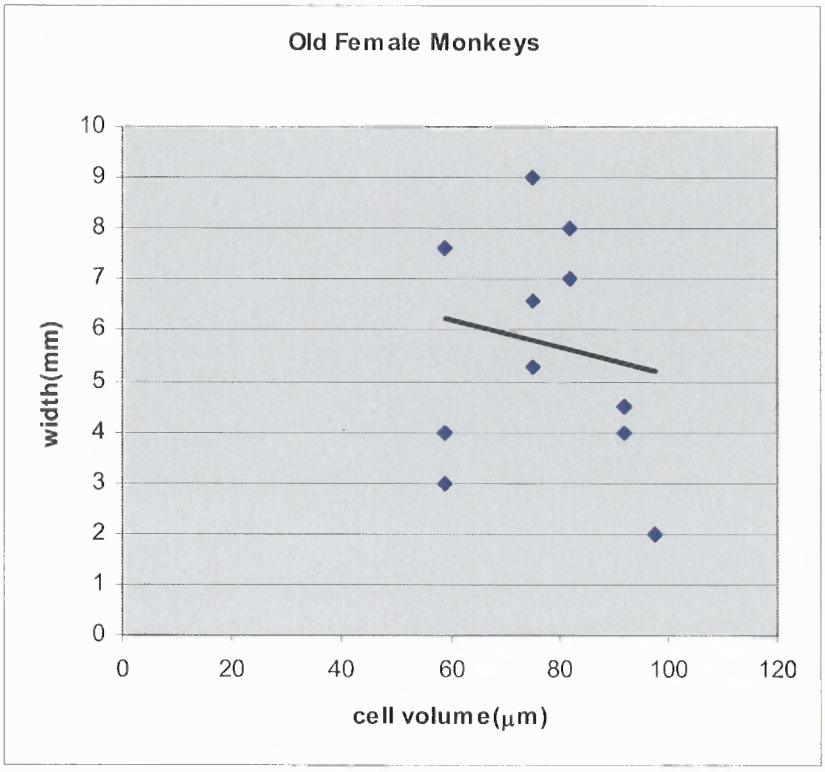

Figure 3.6 Width as a function of cell volume

3.3 Mechanical Testing

The ring was mounted on a triangular hook and a horizontal bar. They are in turn connected to the isometric transducer and sliding element, respectively. The ring is uniaxially stretched with increments of 0.5 mm. With every increment the corresponding force values were noted down and Cytochalasin D was added to eradicate the cytoskeletal component. The force contribution of vascular smooth muscle cell to the tissue was calculated subtracting the total force of tissue construct from the force contributed by the extracellular matrix. The following figure shows a typical mechanical setup for testing the reconstituted tissue.

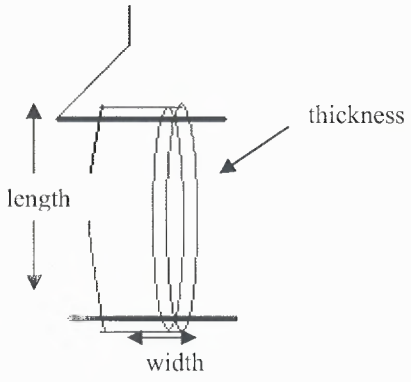

Figure 3.7 Reconstituted tissue mounted on a mechanical system

The stiffness was calculated from stress divided by strain formula. The stress was calculated from the force divided by the cross sectional area.(CSA). From the figure given above the CSA was the product of twice the area of thickness and width. The strain is the change in length which is 0.5mm to the original length it was stretched to.

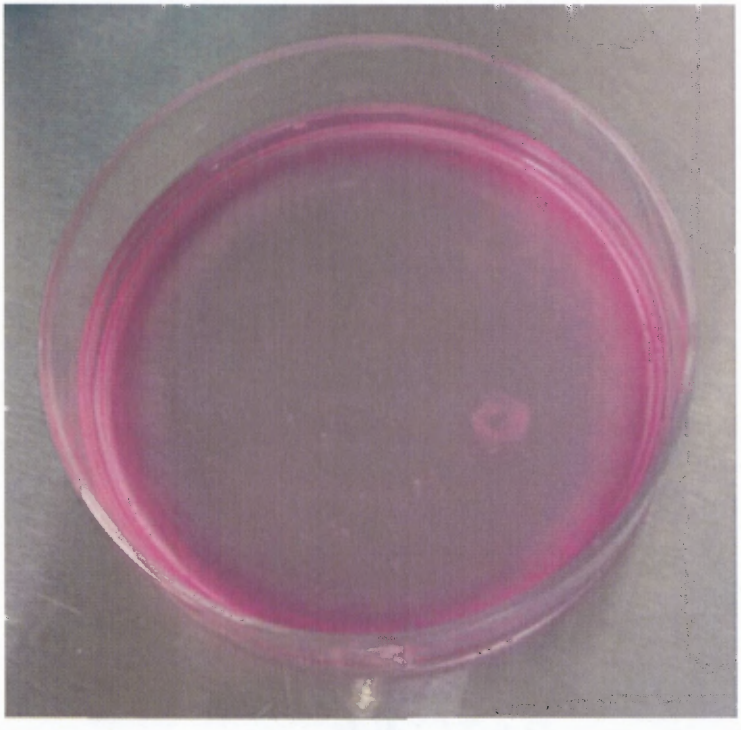

Figure 3.8 Sample of reconstituted tissue that is mounted onto the mechanical system

The reconstituted tissue as seen from above was made to sit on a triangular and horizontal hooks in the diagram described in Figure 3.6 and uniaxially stretched. The force in volts is noted and the Cross Section Area (CSA) computed is used to calculate the stress (force/CSA). Then the stiffness is estimated by change in stress divided by change in strain.

Raw data of NOTOCORD recordings of force with time

Typical force responses to rapid stretches of monkey reconstituted tissue in the young and the old female are presented below. The tissue was suddenly stretched 3 times at intervals of approximately 2 minutes with an increment of 0.5mm .

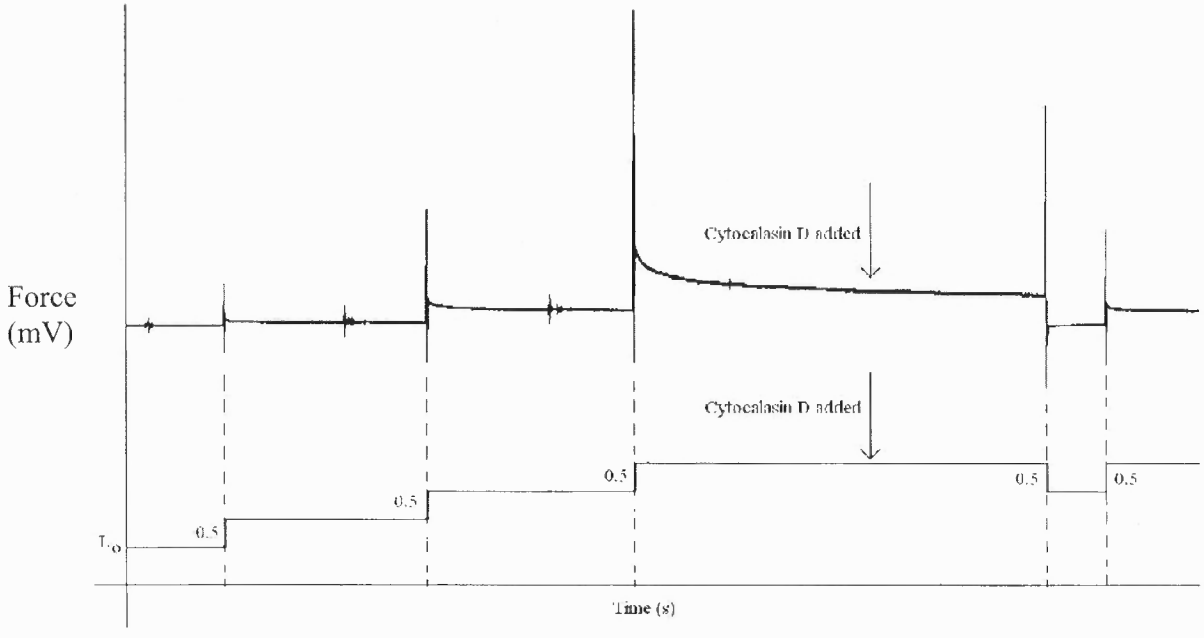

Figure 3.9 Recordings of the force response to rapid stretch of tissue from old female monkeys. After Cytochalasin D treatment, the force was reduced.

Then the Cytochalasin D is added and the reduced force response which indicates the contribution of VSMC to stiffness and stress is calculated. This gives us the Passive component corresponding to Extracellular Matrix(ECM) after the cytoskeletal components were eliminated. The difference between the Total Force (just before CD is added) and the Passive Force (after the CD was added) gives us the Active component, which is computed as described in this study earlier.

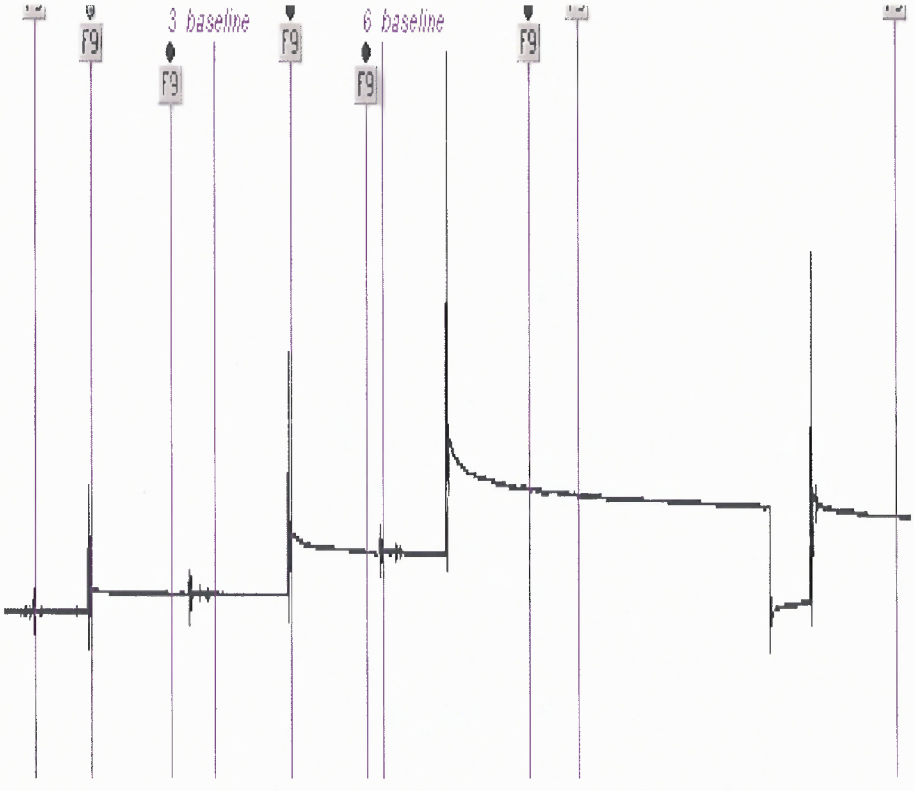

Figure 3.10 Recordings of the force response to rapid stretch of tissue from old female monkeys. After Cytochalasin D treatment, the force was reduced

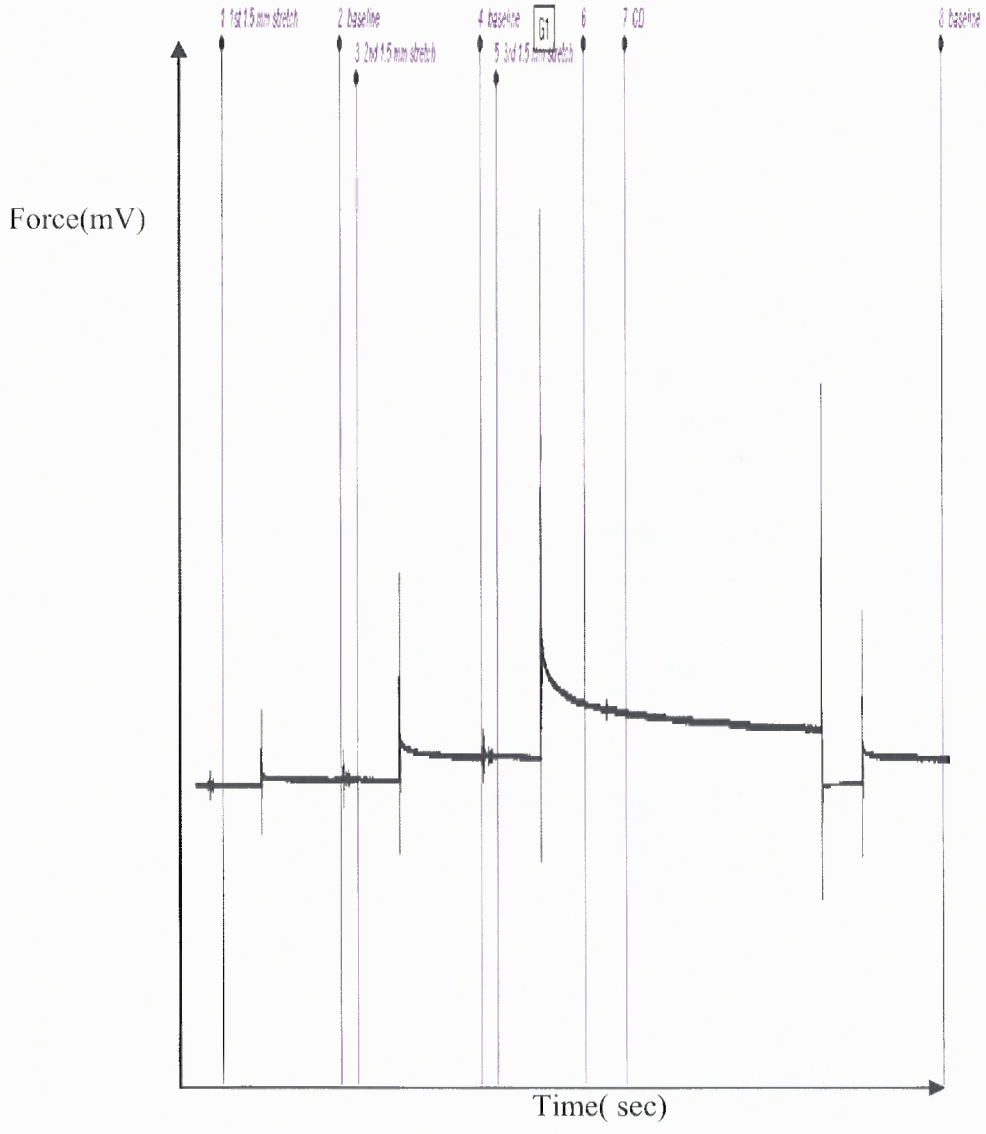

Figure 3.11 Recordings of the force response to rapid stretch of tissue from young female monkeys. After Cytochalasin D treatment, the force was reduced

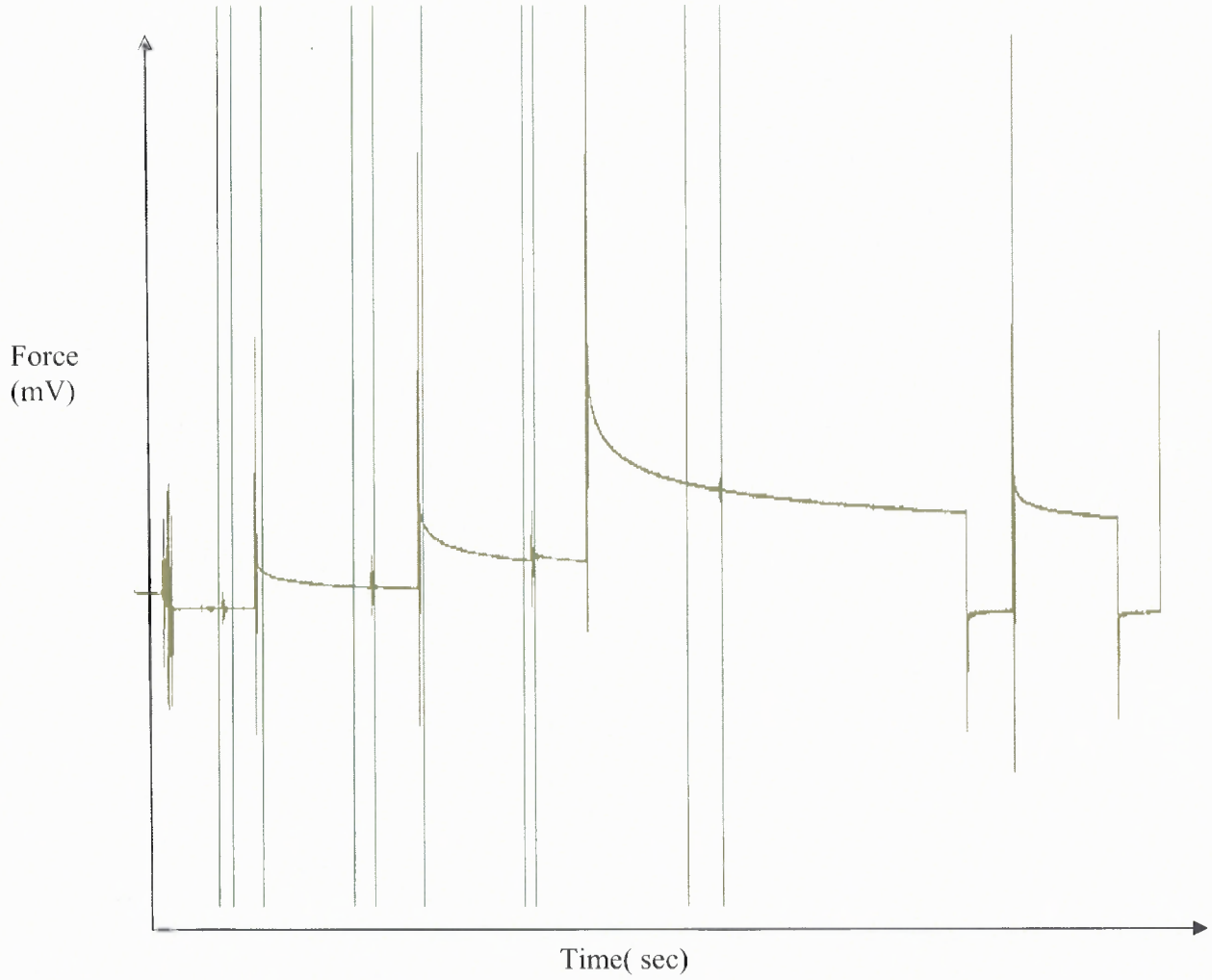

Figure 3.12 Recordings of the force response to rapid stretch of tissue from young female monkeys. After Cytochalasin D treatment, the force was reduced

The following tables and figures below present a quantitative stiffness comparison between the old and young female monkeys with respect to the contributions made by the reconstituted tissue, extracellular matrix and the Vascular Smooth Muscle Cells (VSMCs).

3.3.1 Contribution of Total Stiffness to a Reconstituted Tissue

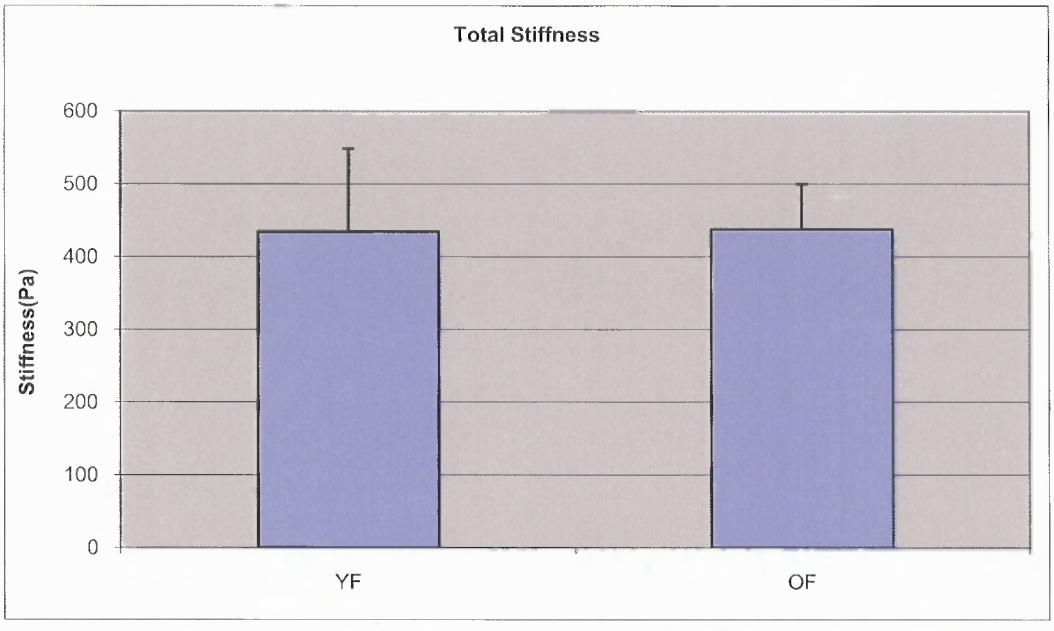

Figure 3.13 Comparison of Total Stiffness between Young Females and Old Females

The total stiffness of the cell contributes to the stiffness measured of the reconstituted tissue as a whole. The stiffness of the reconstituted tissue is the sum of two components, termed "Active" and "Passive". The total stiffness is calculated just before Cytochalasin D is added to the ring. In this study there is no significant difference between the young and old total stiffness. The results shown in Table 3.9 below indicate that there is no significant difference in the total stiffness contributed from reconstituted tissue, the mean values further support our statement.

Table 3.9 Results of Student t-test for total stiffness between young and old females

	Stress(Pascals)	Strain	Total Stiffness(Pa)	n	Mean	SE	sqrt n	P value
YF	130.67	0.14	914.67	1.00	868.93	228.50	2.83	
	58.80	0.14	411.60	2.00				
	32.67	0.14	228.67	3.00				
	261.33	0.14	1829.33	4.00				
	130.67	0.14	914.67	5.00				
	39.20	0.14	274.40	6.00				
	130.67	0.07	1829.33	7.00				
	78.40	0.14	548.80	8.00				
								0.98
OF								
	89.09	0.14	623.64	1.00	875.97	124.28	3.46	
	43.56	0.14	304.89	2.00				
	147.92	0.14	1035.47	3.00				
	196.00	0.14	1372.00	4.00		YF	OF	
	196.00	0.14	1372.00	5.00		868.93	875.97	
	147.00	0.14	1029.00	6.00				
	77.37	0.14	541.58	7.00				
	98.00	0.14	686.00	8.00				
	174.22	0.14	1219.56	9.00				
	147.00	0.14	1029.00	10.00				

3.3.2 Contribution of Extracellular Matrix to a Reconstituted Tissue

As discussed in the above section, the total stiffness is the sum of Active and Passive components. The latter represents the mechanical properties of reconstituted tissue from which cytoskeletal elements have been eliminated by eradicating the actin filaments although a residual amount of cell elements are still remaining from previous studies[ref]. The stiffness and stress of matrix are influenced by the remodeling process, occurring even after the cells are largely eliminated by a biochemical agent CytochalasinD(CD).

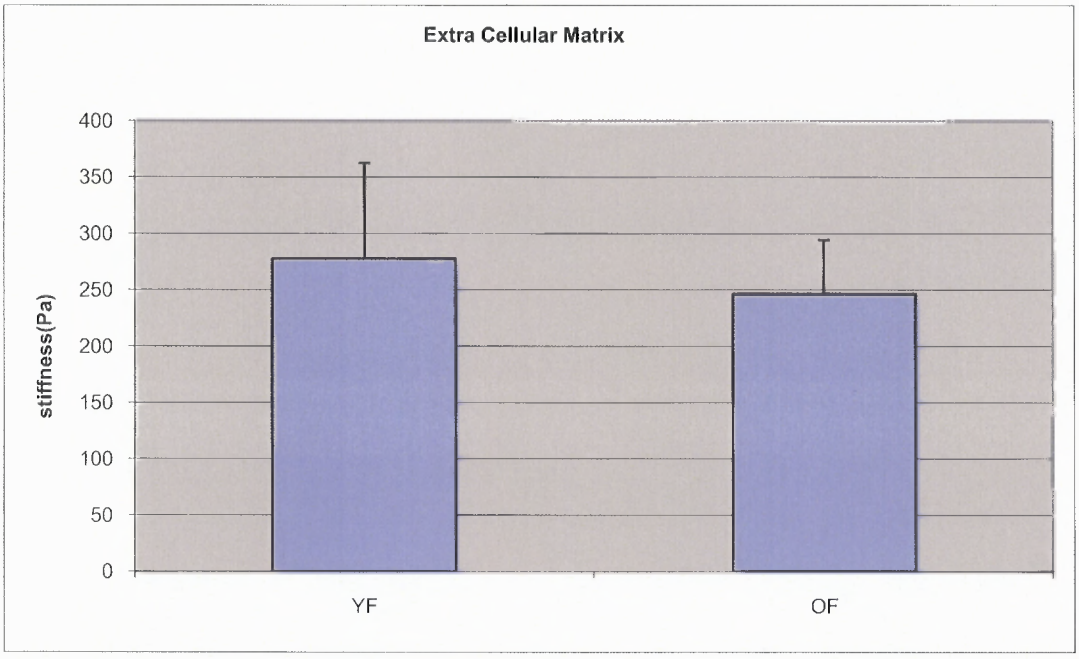

Figure 3.14 Comparison of ECM Stiffness between Young Females and Old Females

The stress is estimated as the force recordings after the treatment of CD divided by the Cross Sectional Area(CSA). The strain is the ratio of change in length (0.5mm) to the original length the tissue was stretched to. i.e., 3.5mm . Therefore the stiffness of the ECM is calculated as the ratio of stress over strain.

Looking over the stiffness contributed by the ECM , Table 3.10 summerizes the "no significant difference" between the young and old female monkeys.

Table 3.10 Results of Student t-test for ECM stiffness between young and old females

	Stress(Pa)	Strain	Ecm Stiffness(Pa)	n	Mean	SE	sqrt n	P value
	87.11	0.14	609.78	1.00	555.47	169.32	2.83	0.74
YF	19.60	0.14	137.20	2.00				
	16.33	0.14	114.33	3.00				
	163.33	0.14	1143.33	4.00				
	87.11	0.14	609.78	5.00				
	26.13	0.14	182.93	6.00				
	98.00	0.07	1372.00	7.00				
	39.20	0.14	274.40	8.00				
	59.39	0.14	415.76	1.00	492.77	95.80	3.46	
OF	21.78	0.14	152.44	2.00				
	73.96	0.14	517.74	3.00				
	98.00	0.14	686.00	4.00		YF	OF	
	130.67	0.14	914.67	5.00		555.47	492.77	
	49.00	0.14	343.00	6.00				
	25.79	0.14	180.53	7.00				
	24.50	0.14	171.50	8.00				
	130.67	0.14	914.67	9.00				
	98.00	0.14	686.00	10.00				
	49.00	0.14	343.00	11.00				
	84.00	0.14	588.00	12.00				

3.3.3 Contribution of Vascular Smooth Muscle Cells to a Reconstituted Tissue

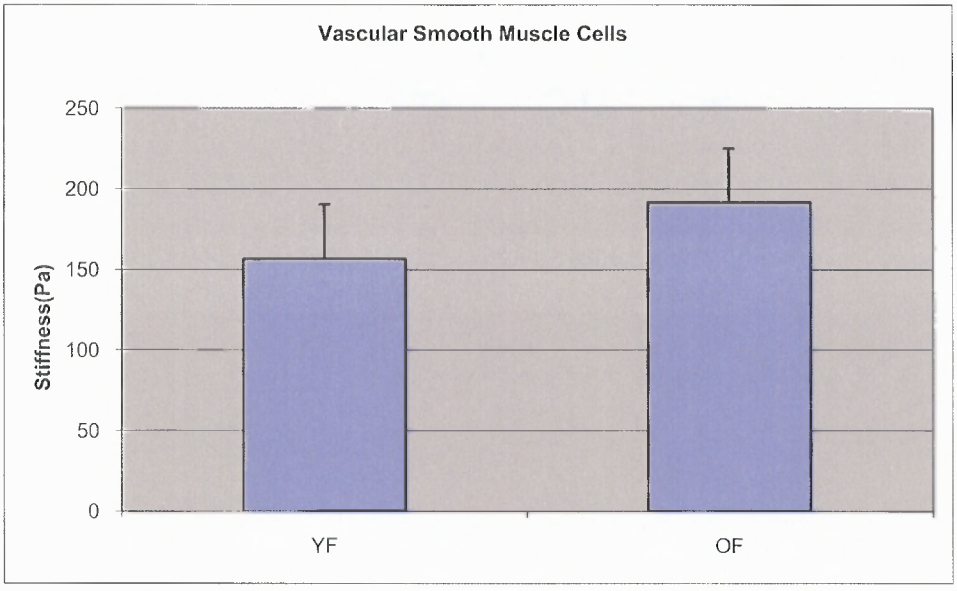

Figure 3.15 Comparison of VSMC Stiffness between Young Females and Old Females

Reiterating from literature survey the VSMCs contribution to the overall stiffness of the reconstituted tissue cannot be directly tested, as the mechanical properties of the cellular components cannot be measured in the absence of the extracellular matrix(ECM) . This is due to the fact that the ECM gives the structural component to the tissue. Hence the state of ECM is directly influenced on the mechanical properties of the active component. We could measure the passive component without the presence of the active component and not vice versa. The values in Table 3.11 summerizes the stiffness contributed by the Vascular Smooth Muscle Cell(VSMCs) calculated from the Total force contribution minus the ECM force contribution.

Table 3.11 Results of Student t-test for VSMC stiffness between young and old females

	Stress(Pa)	Strain	vsmc Stiffness(Pa)	n	Mean	SE	sqrt n	P value
	43.56	0.14	304.89	1.00	313.46	67.03	2.83	0.43
	39.20	0.14	274.40	2.00				
YF	16.33	0.14	114.33	3.00				
	98.00	0.14	686.00	4.00				
	43.56	0.14	304.89	5.00				
	13.07	0.14	91.47	6.00				
	32.67	0.07	457.33	7.00				
	39.20	0.14	274.40	8.00				
	29.70	0.14	207.88	1.00	383.19	67.11	3.46	
	21.78	0.14	152.44	2.00				
OF	73.96	0.14	517.74	3.00				
	98.00	0.14	686.00	4.00		YF	OF	
	65.33	0.14	457.33	5.00		313.46	383.19	
	98.00	0.14	686.00	6.00				
	51.58	0.14	361.05	7.00				
	73.50	0.14	514.50	8.00				
	43.56	0.14	304.89	9.00				
	49.00	0.14	343.00	10.00				
	24.50	0.14	171.50	11.00				
	28.00	0.14	196.00	12.00				

The VSMC contribution to stiffness between the old and the young female has no significant difference. This is the central idea around which this whole study was gone about. Since there is no significant difference seen in the young and old females, goes to show that there is an important parameter within the female mammals that may contribute to this less difference in stiffness between the young and old females.

3.3.4 Stress vs Strain Graph

The mechanical properties of the model tissues are better expressed in terms of stress.

The stress was calculated from force recordings divided by the cross sectional area (CSA).

Table 3.12 Results for stress as a function of change in length in Old Females

Stresses(Pa)			
Initial	1st stretch	2nd stretch	3rd stretch
21.72	21.44	21.67	22.16
10.70	12.27	14.60	16.15
52.43	51.62	52.43	52.11
324.47	298.97	288.33	285.27
183.04	177.52	170.61	159.66
44.81	46.02	48.06	56.77
45.81	60.76	70.20	73.48
32.21	41.37	51.81	52.21
143.77	176.49	191.63	153.02
70.16	63.58	62.22	60.14
14.31	14.77	15.15	15.48
15.99	17.26	15.42	19.85

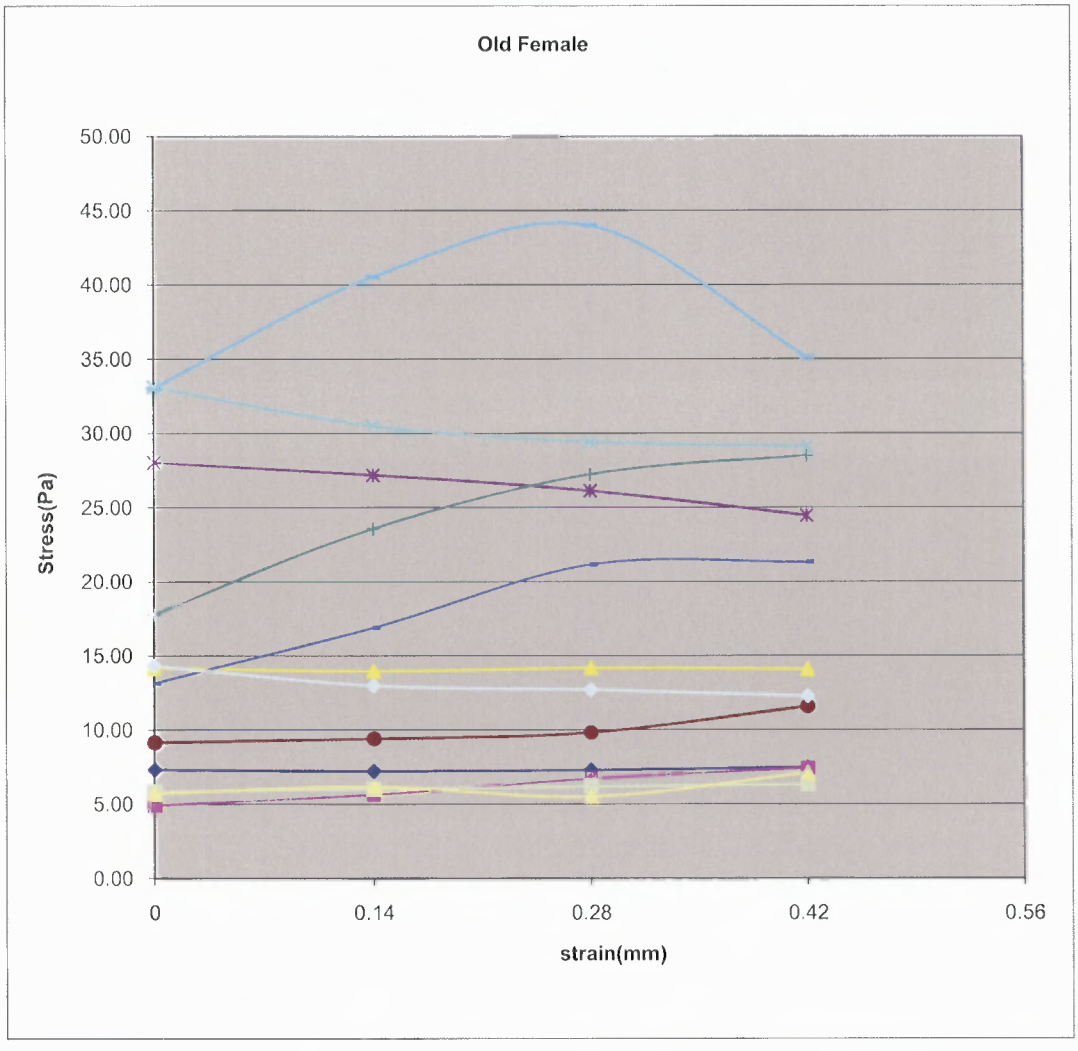

Figure 3.16 Stress as a function of change in length in old females

Table 3.13 Results for stress as a function of strain in Young Females

Stresses			
Initial	1st	2nd	3rd
3.88	6.03	7.45	9.97
17.41	20.22	18.75	23.69
7.80	9.42	11.04	12.65
7.38	7.73	8.41	21.60
5.54	6.37	7.04	7.95
3.46	4.11	4.68	5.36
76.17	95.40	139.93	146.50
24.63	28.84	33.40	37.43

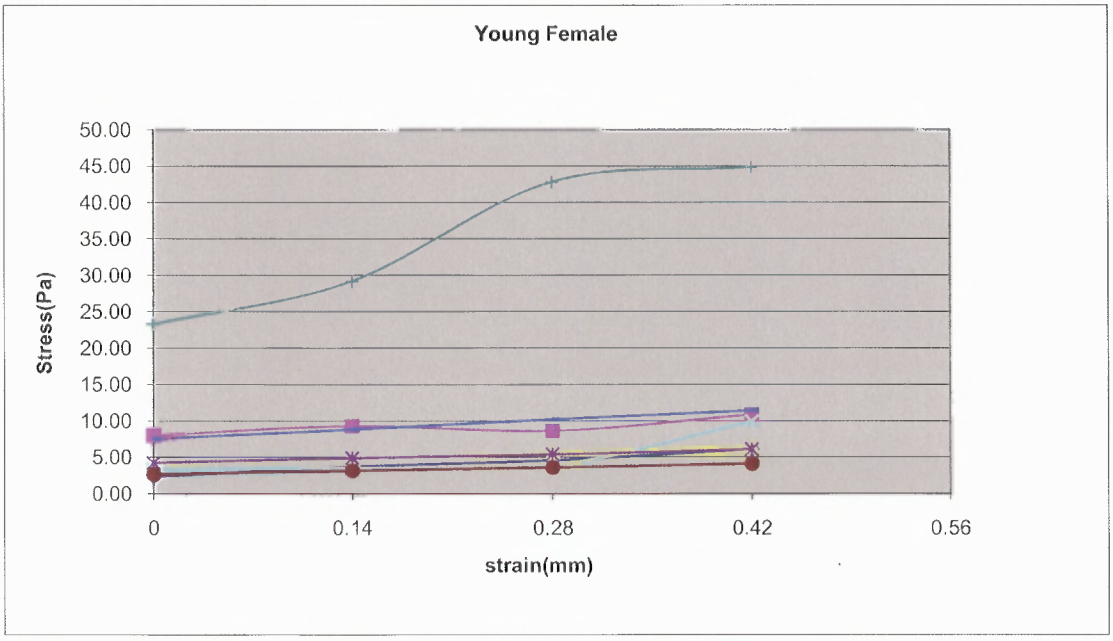

Figure 3.17 Stress as a function of change in length in young females

The Table above summarizes the consequent stress values at various strains of the young female monkey.

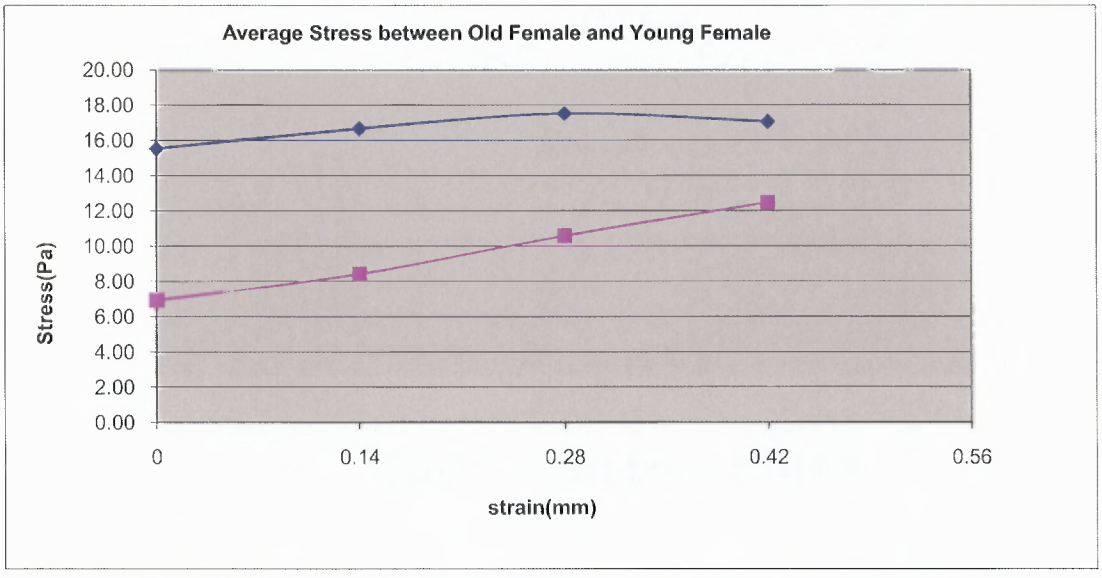

Figure 3.18 Average stress as a function of change in length in young and old females

The figure above shows the stress as a function of strain. As observed from the graph the stress for both the young and the old females increased as the tissue reconstitute

was stretched each time. However the average stress of the young female was comparatively lower than the old female. This goes to show that with age there is increased stress acting on the old females than young ones.

CHAPTER 4

CONCLUSIONS, DISCUSSION AND FUTURE WORK

4.1 Conclusions

We have shown here that tissue constructs consisting of a single cell type and matrix component are a useful system in which to explore tissue, matrix, and cell mechanics. The mechanical properties of reconstituted tissue can be simply characterized using a method explained in this study, which is simple and reproducible.

We employed a method of loading and unloading the reconstituted tissue by uniaxially stretching them by 0.5 mm at constant intervals. After repeated sudden steps, cytochalasin D (CD) was added, which depolymerizes actin within the cells and thus eliminates the cellular contribution to stiffness. The difference in force between that exhibited by the total construct (just before the CD was added) and the passive force exhibited by the matrix alone (after CD eliminated cell stiffness) allowed us to assess the contribution to stiffness from the cells themselves.

The results obtained have suggested that the stiffness contributed by the vascular smooth muscle cell to the overall tissue mechanics for young and old females is not significantly different. Previous studies[13] showed that the stiffness between for vascular smooth muscle cells for young and old male monkeys were drastically different. This is a different result seen here with aging in female monkeys. This difference could be attributed to the presence of the hormone estrogen in females which may exert a protective effect counteracting the effects of aging otherwise seen in male monkeys.

4.2 Discussion

The reconstituted tissue that we have studied has undergone a phase of compression, stiffening and force development over 1-2 days in culture. However slower changes in the mechanics of the tissues cover over a period of time due to cell reorientation and extracellular cross linking.

The aim of this study is to focus on the contribution of vascular smooth muscle cell stiffness in tissue constructs. It employs a novel approach where single cell types from old and young animals are seeded into collagen gel to reconstitute a tissue model. However it has been useful to use different volumes for young and old and yet not make a difference is the overall behavior between the young and old monkeys. By doing so the cell density within the young cells has gone down to attribute to the high proliferative power among the young cells. Using lower volume in the old attributes to old cells undergoing senescence, thereby keeping the mechanics in some way counterbalanced between the young and old. The compliance of the reconstituted tissue observed in this study showed ~0.5kPa whereas in the intact tissue , it is >3.5kPa.

4.3 Future Work

In the future, an image analysis program could be performed in finding the thickness of the tissue construct. Due to the strict protocol of not being able to calculate the thickness, it was assumed to be a constant in both the old and young female monkeys. Once the thickness is calculated, correlations with the width and cell volume with respect to thickness could be made, throwing light into the mechanics of tissue for our better understanding in the future. The need to study the stiffness of single cell as opposed to

whole cell contribution within the reconstituted tissue is crucial as this takes away the bias of young cells proliferating and old female cells undergoing senescence and throws more light into absolute stiffness contribution of single cells eliminating to a larger extent added variables. A thorough histology of cell count and cell density in tissue constructs could be carried out. The need of the hour to study mechanics is driven by the long term goal of engineering tissue constructs to mimic the environment for tissue regeneration with a potential to replace the damaged organs.

Improved methods to expand the cell population of old cells would be helpful. It would also be advisable to perform mechanical preconditioning tests, by stretching the constructs over several cycles before taking measurements. The stiffness observed in these studies is considerably less than the values seen for intact tissue, so means to enhance tissue stiffness might need to be considered. It could also prove informative to make a construct that uses only collagen rings, which could be studied as a negative control test. Histological tests could also be applied to characterize the cells in the reconstituted tissue: for example, staining the nucleus to find out the cell density, seeing how the cells integrate into the collagen network, and using actin staining to confirm loss of actin fibers following the addition of cytochalasin D.

APPENDIX A

PARAMETERS ESTIMATED FROM PREVIOUS PUBLICATIONS[8, 10]

Table A.1 DATA TABULATED FOR GIVEN SET OF PARAMETERS

Cell Parameter	Cell Type	Value	Reference
Cell force	Human small artery	0.1–2 nN	Intengan et al. (1999)
	Leukocyte*	0.8 nN	Evans and Young (1989)
	Fibroblast	500 nN	Kolodney and Wysolmerski (1992)
	Fibroblast	1000 nN	Wakatsuki et al. (2000)
	Active skeletal muscle†	12,500 nN	Ford et al. (1981)
Elastic modulus	Leukocyte (k_p, k_c)	(1.1, 36) Pa	Sung et al. (1988)
	Leukocyte	0.3–0.9 kPa	Zahalak et al. (1990)
	Fibroblast (cortex)	0.06–0.12 MPa	Bausch et al. (1999)
	Single smooth muscle	1.2 MPa	Glerum et al. (1990)
	Fibroblast	2.5 MPa	Wakatsuki et al. (2000)
	Active skeletal muscle‡	20 MPa	Ford et al. (1981)
Cell viscosity	Leukocyte	33 Pa-s	Sung et al. (1988)
	Leukocyte	200 Pa-s	Evans and Young (1989)
	Fibroblast	200 Pa-s	Bausch et al. (1999)
	Active skeletal muscle§	0.26 MPa-s	Katz (1939)

*Estimated from cortical tension.
†With dimensions of a fibroblast.
‡Estimated from T_2 response.
§Estimated from force-velocity relation in stretch.

Table A.2 DATA TABULATED FOR ESTIMATED ELASTIC MODULUS[8]

Cell	Elastic Modulus (MPa)	Reference
Single smooth muscle	6.8	Harris and Warshaw (1991)
Single smooth muscle	1.2	Glerum et al. (1990)
Single CEF	0.001	Thoumine and Ott (1997)
CEF	2.5	This work

Table A.3 DATA TABULATED FOR ESTIMATED ELASTIC MODULUS[8]

Type of tissue	Elastic Modulus (MPa)	Reference
Tendo achillis	375	Lewis and Shaw (1997)
Human knee menisci	73–151 (circumferential)	Tissakht and Ahmed (1995)
Human knee menisci	30–60 (radial)	Tissakht and Ahmed (1995)
Human brachial artery	4	Bank and Kaiser (1998)
Human small artery	0.1–2	Intengan et al. (1999)
FPM*	0.08–0.24	Chapuis and Agache (1992)
Collagen sponge	0.017–0.028	Jain et al. (1990)
FPM	0.8	This work

*0.65 mg/ml collagen, 57,000 cells/ml.

Table A.4 DATA TABULATED FOR ESTIMATED FORCE VALUES[8]

Cell	Force (nN/cell)	Reference
Smooth muscle*†	1500	Harris and Warshaw (1991)
Keratocytes*‡	48	Oliver et al. (1995)
Fibroblasts*§	52	Roy et al. (1999)
Fibroblasts*¶	40	Thoumine and Ott (1997)
Fibroblasts*‖	1–3 (nN/μm^2)	Galbraith and Sheetz (1997)
Fibroblasts**	500	Kolodney and Wysolmerski (1992)
Fibroblasts**	0.1	Eastwood et al. (1996)
Fibroblasts	1000	This work

*Force is measured by a single cell manipulation.
Force is measured by †force transducer, ‡silicon substratum, §collagen substratum, ¶microplates, ‖nano-fabricated substratum.
**Force is estimated from the contractile force produced by FPMs.

REFERENCES

[1] F. Grinnell, "Fibroblasts, myofibroblasts, and wound contraction," *The Journal of cell biology,* pp. 401-404, 1994.

[2] I. Mackenzie, *et al.*, "Assessment of arterial stiffness in clinical practice," *Qjm,* vol. 95, p. 67, 2002.

[3] M. E. Safar, *et al.*, "Arterial stiffness and kidney function," *Hypertension,* vol. 43, p. 163, 2004.

[4] P. B. Dobrin, "Mechanical properties of arteries," *Physiol Rev,* vol. 58, pp. 397-460, 1978.

[5] M. Safar, *et al.*, "Current perspectives on arterial stiffness and pulse pressure in hypertension and cardiovascular diseases," *Circulation,* vol. 107, p. 2864, 2003.

[6] S. Laurent, *et al.*, "Aortic stiffness is an independent predictor of all-cause and cardiovascular mortality in hypertensive patients," *Hypertension,* vol. 37, p. 1236, 2001.

[7] Z. Feng, *et al.*, "Measurements of the mechanical properties of contracted collagen gels populated with rat fibroblasts or cardiomyocytes," *Journal of Artificial Organs,* vol. 6, pp. 192-196, 2003.

[8] T. Wakatsuki, *et al.*, "Cell mechanics studied by a reconstituted model tissue," *Biophysical Journal,* vol. 79, pp. 2353-2368, 2000.

[9] J. J. Wille, *et al.*, "Cellular and matrix mechanics of bioartificial tissues during continuous cyclic stretch," *Annals of biomedical engineering,* vol. 34, pp. 1678-1690, 2006.

[10] G. Zahalak, *et al.*, "A cell-based constitutive relation for bio-artificial tissues," *Biophysical Journal,* vol. 79, pp. 2369-2381, 2000.

[11] B. Jennifer, *et al.*, "Tensile Mechanical Properties of Three-Dimensional Type I Collagen Extracellular Matrices With Varied Microstructure," *Journal of Biomechanical Engineering,* vol. 124, 2002.

[12] G. Wood and M. Keech, "The formation of fibrils from collagen solutions 1. The effect of experimental conditions: kinetic and electron-microscope studies," *Biochemical Journal,* vol. 75, p. 588, 1960.

[13] A. Veis and A. George, "Fundamentals of interstitial collagen selfassembly," *Extracellular Matrix Assembly and Structure,* p. 15, 1994.

[14] S. Voytik-Harbin, "Three-dimensional extracellular matrix substrates for cell culture," *Methods in cell biology,* vol. 63, p. 561, 2001.

[15] Wikipedia. (2004, *Lumen (anatomy).*

[16] NOVOGEN. (2010, *Cardiovascular Program* [Company Based Website].

[17] J. Wagenseil, *et al.*, "One-dimensional viscoelastic behavior of fibroblast populated collagen matrices," *Journal of Biomechanical Engineering,* vol. 125, p. 719, 2003.

[18] T. Eschenhagen, *et al.*, "Three-dimensional reconstitution of embryonic cardiomyocytes in a collagen matrix: a new heart muscle model system," *The FASEB Journal,* vol. 11, p. 683, 1997.

[19] T. Wakatsuki and E. L. Elson, "Reciprocal interactions between cells and extracellular matrix during remodeling of tissue constructs," *Biophysical Chemistry,* vol. 100, pp. 593-605, 2003.

[20] D. E. V. Stephen F Vatner, Hongyu Qiu et al, "Age and Gender Effects on Cardiovascular Function in Primates," University of Medicine and Dentistry of New Jersey, Newark ,NJ July 2007.

[21] H. Qiu, *et al.*, "Regional Difference of Increased Stiffness and Extra Cellular Matrix in Aging Monkey Aorta," *The FASEB Journal,* vol. 23, p. 774.10, 2009.

[22] H. Qiu, *et al.*, "Sex-specific regulation of gene expression in the aging monkey aorta," *Physiological Genomics,* vol. 29, p. 169, 2007.

[23] C. Protocols. (2007, 13th January 2010). *Cell Subculture Protocol.*

[24] J. P. Marquez, *et al.*, "The relationship between cell and tissue strain in three-dimensional bio-artificial tissues," *Biophysical Journal,* vol. 88, pp. 778-789, 2005.